

An Abstract of the Thesis of

Peggy Ann Dalheim for the degree of Master of Science
in the Department of Geology to be taken September, 1977

Title: CALCULATION OF EMPIRICAL CORRELATION COEFFICIENTS IN MULTI-COMPONENT OXIDE SYSTEMS FOR THE REDUCTION OF ELECTRON MICRO-PROBE DATA.

Approved: Daniel F. Weill
(Daniel F. Weill)

The purpose of this project was twofold - to synthesize several electron microprobe glass standards in the system: $\text{SiO}_2 - \text{Al}_2\text{O}_3 - \text{CaO} - \text{MgO}$, and to utilize these standards in empirically calculating a set of binary correlation coefficients for use in the Bence-Albee data reduction method. Ten standards were prepared using the four end member oxides in coarse, crystalline form as starting materials (99.9⁺% purity). The careful synthesis and extensive analysis of the standards insured that they are homogeneous with compositions known to better than 5×10^{-4} oxide weight percent. The X-ray intensities measured for Si, Al, Ca and Mg in the standards and the oxides, plus the known compositions of the glasses provided the information necessary to empirically derive the set of binary correlation coefficients ("alpha factors") within the $\text{SiO}_2 - \text{Al}_2\text{O}_3 - \text{CaO} - \text{MgO}$ system.

CALCULATION OF EMPIRICAL CORRELATION COEFFICIENTS IN
MULTICOMPONENT OXIDE SYSTEMS FOR THE REDUCTION
OF ELECTRON MICROPROBE DATA

by

Peggy Ann Dalheim

FOUR STAR BOND
SOUTHWORTH CO. U.S.A.
292 CUMBER RIDGE

A THESIS

Presented to the Department of Geology and the
Graduate School of the University of Oregon
in partial fulfillment of the
requirements for the degree of
Master of Science

September, 1977

APPROVED: *Daniel F. Weill*
(Daniel F. Weill)

FOUR STAR BOND
SOUTHWORTH CO. U.S.A.
25% COTTON FIBER

VITA

NAME OF AUTHOR: Peggy Ann Dalheim

PLACE OF BIRTH: Troy, New York

DATE OF BIRTH: September 14, 1951

UNDERGRADUATE AND GRADUATE SCHOOLS ATTENDED:

State University of New York at Albany
University of Oregon

DEGREES AWARDED:

Bachelor of Science, 1973, State University of New York at Albany

AREAS OF SPECIAL INTEREST:

Geochemistry
Igneous Petrology

PROFESSIONAL EXPERIENCE:

Teaching Assistant, 1974-1976, Geology Department, University of Oregon

AWARDS AND HONORS:

New York State Regents Scholarship, 1969-1973

TABLE OF CONTENTS

	<u>Page</u>
Title Page	i
Approval Page	ii
Vita	iii
Acknowledgments	iv
Table of Contents	v
List of Figures	vii
List of Tables	ix
INTRODUCTION	1
THE MICROPROBE	3
STANDARD SELECTION AND PREPARATION	6
Selection of Mixes	6
Preparation	7
Analysis of Standards	12
CORRECTION TECHNIQUES FOR MICROPROBE DATA REDUCTION	26
ZAF Correction Technique	26
Empirical Correction Techniques	29
Calculation of Alpha Factors	31
Uncertainties in Alpha Factors	44
Variation in Values of Alpha Factors	47

FOUR STAR BOND

SOUTHWORTH CO. U.S.A.

	<u>Page</u>
CONCLUSION	63
Appendix 1. Sample Preparation Notes	64
Appendix 2. Theoretical (ZAF) Correction Method	70
Appendix 3. Data Used in the Linear Least Squares Program and Errors Propagated by that Method	75
Appendix 4. Miscellaneous Data	84
REFERENCES	88

FOUR STAR BOND
SOUTHWORTH CO. U.S.A.
25% COTTON FIBER

LIST OF FIGURES

<u>Figure</u>		<u>Page</u>
1	Quaternary Diagram: $\text{SiO}_2 - \text{Al}_2\text{O}_3 - \text{CaO} - \text{MgO}$	8
2	Poisson Distributions Compared with Observed Count Distributions for Four Elements in Mix B	14
3	Histograms of Microprobe Data for "Perfectly Homogeneous" and "Inhomogeneous" Samples	24
4	Theoretical Binary Alpha Factors Involving Al_2O_3 and SiO_2	41
5	Theoretical Binary Alpha Factors Involving SiO_2 and MgO	41
6	Theoretical Binary Alpha Factors Involving CaO and Al_2O_3	42
7	Theoretical Binary Alpha Factors Involving Al_2O_3 and MgO	42
8	Theoretical Binary Alpha Factors Involving MgO and CaO	43
9	Theoretical Binary Alpha Factors Involving CaO and SiO_2	43
10	Theoretical and Empirical Distributions for ^{29}Si $^{29}\text{Si-MgO}$	50
11	Theoretical and Empirical Distributions for ^{27}Al $^{27}\text{Al-SiO}_2$	50
12	Theoretical and Empirical Distributions for ^{40}Ca $^{40}\text{Ca-SiO}_2$	51
13	Theoretical and Empirical Distributions for ^{40}Ca $^{40}\text{Ca-Al}_2\text{O}_3$	51

<u>Figure</u>		<u>Page</u>
14	Theoretical and Empirical Distributions for Si $\alpha\text{-Si-Al}_2\text{O}_3$	52
15	Theoretical and Empirical Distributions for Si $\alpha\text{-Si-CaO}$	52
16	Theoretical and Empirical Distributions for Mg $\alpha\text{-Mg-Al}_2\text{O}_3$	53
17	Theoretical and Empirical Distributions for Mg $\alpha\text{-Mg-CaO}$	53
18	Theoretical and Empirical Distributions for Ca $\alpha\text{-Ca-MgO}$	54
19	Theoretical and Empirical Distributions for Mg $\alpha\text{-Mg-SiO}_2$	54
20	Theoretical and Empirical Distributions for Al $\alpha\text{-Al-CaO}$	55
21	Theoretical and Empirical Distributions for Al $\alpha\text{-Al-MgO}$	55
22	Theoretical and Empirical Distributions for Si $\alpha\text{-Si-MgO}$ with Mix J Excluded from the Set of Exact Solutions of Three Linear Equations	58

LIST OF TABLES

<u>Table</u>		<u>Page</u>
1	Results of Analysis of Ten Mixes at 15 KV by the Bence-Albee Method	9
2	Homogeneity Data for the Ten Glasses	18
3	Alpha Factors Calculated by Several Methods at 15 KV	45
4	T α and E α Factors Calculated at 10 KV, 20 KV, 30 KV	46
5	Error Reduction Caused by Elimination of One Mix from the Least Squares Solution at 15 KV .	48
6	Comparison of Standard Deviations by Least Squares Method and Method Two	56
7	Differences (in %) in Compositions as Predicted by Various Sets of Alpha Factors at 15 KV	60
8	Sets of Alpha Factors Which Show the Average Lowest Difference (from Table 7) for Individual Oxides	62
9	Empirical Alpha Factor Data (15 KV) Used in Solution of Ten Linear Equations	76
10	Empirical "B" Used in Solution of Ten Linear Equations by Least Squares Method at 10, 20, and 30 KV	77
11	Theoretical Alpha Factor Data at 10, 15, 20, and 30 KV Used in Linear Least Squares Solutions of Ten Equations	78
12	Standard Deviations (σ) of the Twelve Empirical Alpha Factors Propagated by the Least Squares Solution of Ten Equations (15 KV)	79

<u>Table</u>		<u>Page</u>
13	Standard Deviations (σ) of the Twelve Empirical Alpha Factors Propagated by the Least Squares Solution of Ten Equations (10 KV)	80
14	Standard Deviations (σ) of the Twelve Empirical Alpha Factors Propagated by the Least Squares Solution of Ten Equations (20 KV)	81
15	Standard Deviations (σ) of the Twelve Empirical Alpha Factors Propagated by the Least Squares Solution of Ten Equations (30 KV)	82
16	Standard Deviations (σ) of the Twelve Theoretical Alpha Factors Propagated by the Least Squares Solution of Ten Equations (15 KV)	83

INTRODUCTION

The Electron Microprobe has become an important tool in the quantitative analysis of rocks and minerals in the relatively short time since its conception in the late 1940's by Castaing and Guinier (1949). The probe enables researchers to study in-situ mineral relations on a micron scale. Whole rock analyses may also be done using fused rock powders. The importance of the probe as an analytical tool requires that critical examinations of data gathering and data reduction techniques be made. These examinations entail the study of machine design, operating conditions, standard preparation, and data reduction methods.

The purpose of this project has been to produce several "reliable" standards of significance to silicate systems and to critically examine one method of data reduction - the Bence-Albee method. Quantitative microprobe analysis is a comparative technique (as are all X-ray methods of analysis). X-ray intensities produced by known standards are compared to X-ray intensities produced by the unknown. The ratio of standard X-ray intensity for a particular element to X-ray intensity for that same element in the unknown is approximately equal to the ratio of weight concentration of that element in the standard to concentration in the unknown. If the standard is exactly the composition of the unknown, these ratios should be equal. Since this is rarely the case, theoretical or empirical factors are employed to

correct the intensity ratio. To minimize the correction factor, the standards should be close in composition to the unknowns.

A four component system was chosen to study in this project - SiO_2 , Al_2O_3 , CaO and MgO . The combination of these four oxides comprises approximately 80% by weight of most rocks and constitutes a significant portion of many minerals. Therefore, glasses in this four component system provide valuable microprobe standards for geologists. The glass standards produced were used to refine the Bence-Albee data reduction method. The Bence Albee technique employs empirical matrix correction factors that are essentially weighted averages of binary oxide correction factors. These factors reflect the effect of one element or oxide upon the X-ray intensity of another element. Several glasses within the four component system were used to re-determine these correction factors. The following report describes the analytical instrument used, the method of glass preparation, the Bence-Albee method and the use of carefully prepared glasses to refine this empirical data reduction method.

THE MICROPROBE

A basic appreciation of the instrument is pertinent to the understanding of standard selection and preparation, and data reduction techniques. The electron microprobe consists principally, of an electron source, a series of de-magnifying electro-magnetic lenses, a viewing system - usually a polarizing and/or reflecting microscope, electron detectors, X-ray detectors, and a means of converting X-ray intensity (or electron signal) to a digital readout.

The electron beam column consists of an electron source, lenses and sample stage sealed in a vacuum of less than 10^{-4} torr to minimize electron absorption and scattering by air. The electron source is a hot filament, usually of tungsten wire about 100 microns in diameter. The number of electrons emitted from the filament is proportional to the amount of current flowing through the filament. The grid cap (physically below the filament) is biased negatively with respect to the filament causing the electrons to cross-over approximating focus. The electrons are accelerated toward the anode by a potential of 0 to 30KV. Two electro-magnetic lenses - the condenser and objective lenses are used to de-magnify the source image 100 to 1000 times, allowing a "spot" of approximately 0.2-300 microns to be focused on the surface of a sample. The sample is raised into optical focus by a mechanical stage. The optical focal point and beam focal point are coincident.

Electrons incident on the sample excite X-rays of wavelengths characteristic of the elements in the sample. These X-rays are analyzed by wavelength spectrometers. Three wavelength spectrometers are mounted on the ARL probe used in this project. The spectrometer consists of a diffracting crystal and a sealed or flow proportional counter. The crystal can be mechanically positioned such that specific wavelengths are diffracted according to Bragg's Law:

$$n\lambda = 2d\sin\theta$$

where n is an integer, λ = the wavelength of the X-ray photon, d = the lattice spacing of the crystal, and θ = the angle of incidence of the X-rays on the crystal. The X-ray photons diffracted by the crystal are collected by a gas proportional counter and converted to electrical pulses. The probe uses both flow proportional and sealed proportional counters. X-ray photons enter the counter through a thin detector window of beryllium or mylar. The window must be thin enough to allow X-rays through without significant absorption. For X-rays of wavelength greater than three angstroms, windows must be so thin that they are not gas tight. In this case, gas must constantly flow through the counter. For X-rays less than three angstroms, a thicker window is used; the counter is gas tight or sealed.

Each X-ray photon entering the counter produces a number of ion - electron pairs of the gas (usually Xenon or Argon-methane) proportional to the energy of the photon. The electrons produced are accelerated to a central collection wire maintained at a positive potential of 1000 to 2000 volts. Each accelerated electron causes many other ionizations

(approx. 10^4 such events) so that many electrons strike the wire for each entering photon. The collection of these electrons produces a momentary drop in voltage. This drop and subsequent recovery in voltage produces an electrical pulse. The pulses are amplified and represented on a digital display. The characteristic X-ray intensity (or number of photons) is proportional to the concentration of the element in question. Therefore, the number of pulses per time period is proportional to concentration.

STANDARD SELECTION AND PREPARATION

Selection of Mixes

Standards used in microprobe analysis should closely approximate the chemical composition of phases analyzed (the "unknowns"). Using a standard that closely approximates the unknown minimizes the correction factor required to convert X-ray intensity to concentration. After the raw counts (measure of X-ray intensity) are corrected for background and deadtime, the ratio of the characteristic X-ray intensity produced by the element being analyzed in the unknown to that X-ray intensity measured for the standard is multiplied by a correction factor, f .

That is:

$$(1) \quad C_u^n / C_s^n = (k_u^n / k_s^n) \times f$$

where C_u^n equals the weight concentration of element n in the unknown, C_s^n equals the weight concentration of element n in the standard, k_u^n equals the characteristic X-ray intensity produced by n in the unknown, k_s^n equals the characteristic X-ray intensity produced by element n in the standard, and f is the correction factor. As the composition of the standard approaches the composition of the unknown, f approaches one. For example, if CaSiO_3 (wollastonite) is the unknown, analyzed for Si, three possible Si standards result in the following correction factors (ZAF correction for Si):

<u>Standard</u>	<u>f</u>
Si (metal)	0.8817
(Ca,Mg)SiO ₃	0.9348
CaSiO ₃	1.0000

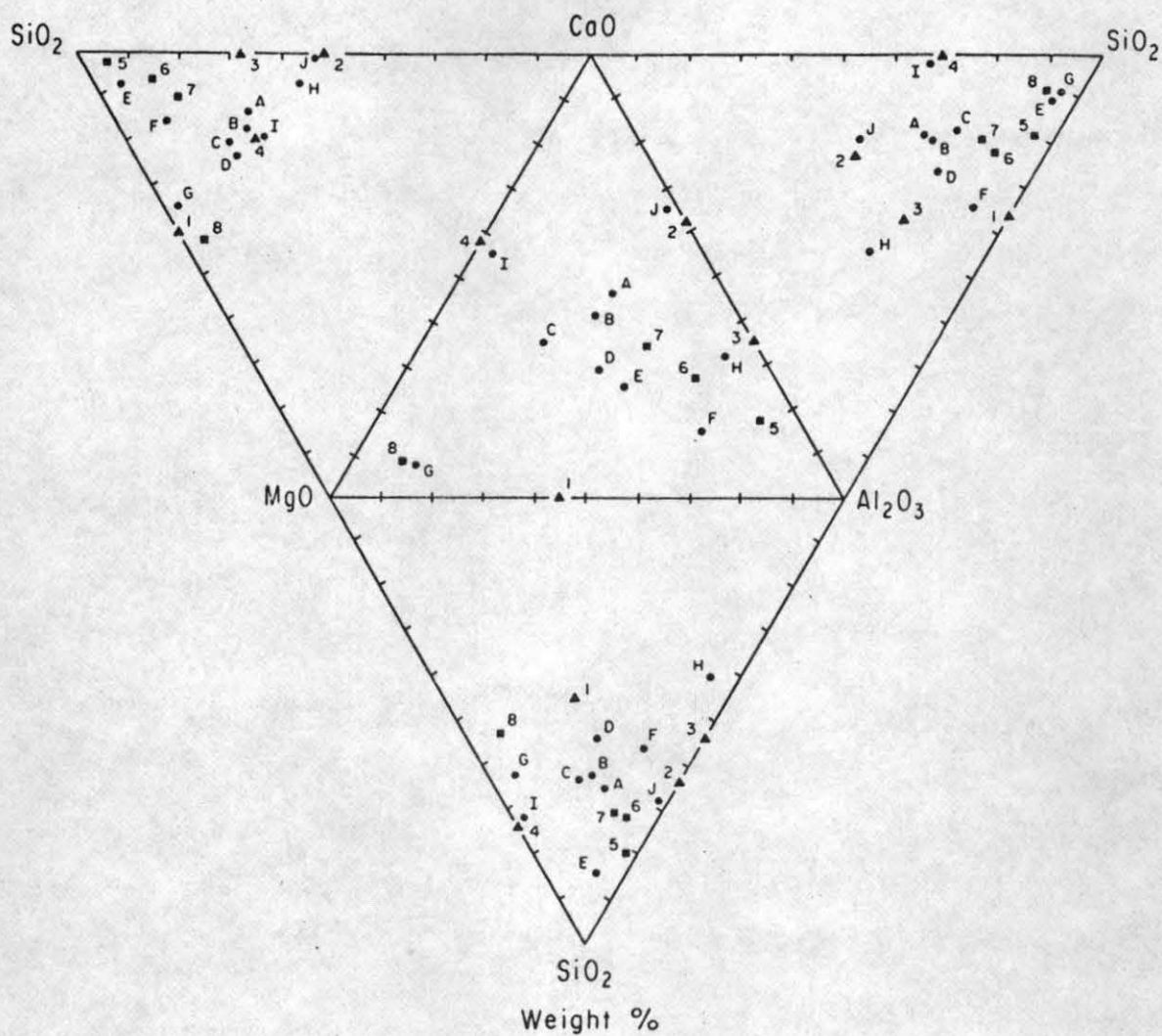
A second example, when Fe₂SiO₄ (fayalite) is the unknown being analyzed for Fe, the correction factors are (Bence-Albee correction for FeO):

<u>Standard</u>	<u>f</u>
Fe ₂ SiO ₄	1.00
FeTiO ₃	1.14
FeO	1.21

Since silicate rocks and minerals are an integral part of geologic study, microprobe standards that closely approximate the major element compositions of rocks and minerals are important to geologists. For this reason, glasses in the system SiO₂ - Al₂O₃ - CaO - MgO were prepared for microprobe standards. Seventy-five to 85% by weight of most igneous rocks and many minerals lie within this system. The ten mixes chosen for preparation are plotted with representative rock and mineral compositions in the quaternary system on Figure 1 and listed in Table 1. These mixes were chosen to encompass the greatest volume within the quaternary system limited by stability and high melting temperatures.

Preparation

The composition of a standard should be well known, i.e., more exactly than can be determined by the microprobe. Most other methods of major element analysis are no more accurate than microprobe analysis.



- | | | |
|--------------------------------|----------------------|------------------|
| 1 - Pyrope | $Mg_3Al_2Si_3O_{12}$ | 5 - Granodiorite |
| ▲ 2 - Grossular | $Ca_3Al_2Si_3O_{12}$ | ■ 6 - Andesite |
| 3 - Anorthite | $CaAl_2Si_2O_8$ | 7 - Basalt |
| 4 - Diopside | $(Mg, Si)_2Si_2O_6$ | 8 - Peridotite |
| ● A thru J - Synthetic Glasses | | |

Figure 1. Quaternary Diagram: $SiO_2 - Al_2O_3 - CaO - MgO$ including the ten mixes and representative rock and mineral compositions.

Table 1. Results of Analysis of Ten Mixes at 15 KV by the Bence-Albee Method
(in weight percent)

Mix	SiO ₂		Al ₂ O ₃		CaO		MgO		B-A Total
	Weighed-in	Probe	Weighed-in	Probe	Weighed-in	Probe	Weighed-in	Probe	
Mix C	52.1275	—	13.9750	—	16.9639	—	16.9336	—	
Mix A	49.7197	49.58	16.0740	16.06	23.1517	23.20	11.0547	11.04	99.87
Mix B	48.9858	48.88	16.0520	16.04	20.9739	21.08	13.9883	13.95	99.95
Mix D	45.0723	45.08	20.9604	20.96	15.9953	16.09	17.9720	18.01	100.14
Mix E	79.9712	77.42	8.9880	9.34	5.0432	5.04	5.9976	5.91	97.71
Mix E*		80.27		9.34		5.04		5.91	100.56
Mix F	52.0609	51.84	30.9256	30.57	6.9410	7.00	10.0725	10.06	99.46
Mix G	61.1182	60.69	3.3063	3.30	2.8875	2.96	32.6880	32.79	99.74
Mix H	30.9072	31.30	41.8957	41.79	21.9741	22.01	5.2230	5.18	100.28
Mix I	52.9524	52.81	2.0056	2.05	26.0093	26.07	19.0327	18.99	99.91
Mix J	42.9757	42.95	19.0180	19.10	36.9943	36.78	1.0120	0.99	99.82

*Mix E analyzed for Si using Quartz (SiO₂) as a standard.

Therefore, it was decided to use weighed-in concentrations of oxides as the "true" composition of the synthetic standards prepared for this project.

Synthetic CaO crystals from Atomergic Chemetals, synthetic periclase (MgO) from Materials Research Corp., synthetic alumina (Al_2O_3 ; sapphire crackle) from Union Carbide and natural quartz (SiO_2) from Ward's Scientific were used as starting materials. All of the oxides were of at least 99.9% purity. The four oxides were analyzed on the microprobe for Ca, Mg, Al and Si. Only MgO showed slightly higher than background counts of a contaminating element - Ca. The manufacturer's analysis of the MgO included 300ppm Ca. Oxide powders were purposely avoided as starting materials for the synthetic glasses because they absorb water (as much as a percent by weight when weighing out several gram (1-5) quantities of MgO). Several steps were taken to avoid this problem. Coarse crystalline oxides were used as starting materials. Obviously, since coarse materials have less surface area per mass than powders, there was less absorption of water. MgO and CaO (CaO is unstable in air) were stored in a vacuum dessicator under an argon atmosphere. Large chunks of these two oxides were broken in a hardened steel cylinder into millimeter (1-3mm) size pieces just before weighing. The Al_2O_3 was particularly difficult to break up into small pieces. It was coarse ground in a tungsten carbide ball mill to approximately one mm size. The Al_2O_3 picked up about one percent by weight tungsten during grinding. The tungsten was removed by soaking the contaminated Al_2O_3 in aqua regia for 24 hours, followed by rinsing in de-ionized

water. The Al_2O_3 was then dried at $200\text{--}300^\circ\text{C}$ for 24 hours and stored in a dessicator (CaSO_4 dessicant) until used. The quartz was broken in an iron mortar and cleaned with concentrated HCl , rinsed with de-ionized water, dried for 24 hours at $200\text{--}300^\circ\text{C}$ and stored with the Al_2O_3 until used. The balance chamber was dessicated before using. CaO , then MgO were weighed out. Each was exposed to the air for the time it took to break the material and weigh it - several minutes. CaO exhibited a slight weight gain during weighing (on the order of 10^{-6} grams). The other three oxides exhibited no such gain.

The third factor in accurate weighing was the accuracy and precision of the balance used. A Mettler, M5, microbalance (sensitivity to 10^{-6} grams) was used. The balance was in a temperature and humidity controlled room. The zero of the balance was checked repeatedly during weighing and did not appear to drift. Two to three mixes were weighed out in a single sitting. The total weighing time was under two hours for each group so possible barometric effects were considered negligible. The balance was repeatable to 1×10^{-5} grams. Mixes weighed either two or five grams. These weights were selected to conserve input materials while minimizing possible weighing errors. No single oxide in any mix weighed less than 0.10 grams. Therefore, the possible error due to weighing in the weight percent of any one oxide in the five gram mixes was no more than 2×10^{-4} ; the possible error in the weight percent of any one oxide in the two gram mixes was no more than 5×10^{-4} . The weighing errors were well below the limit of detectability of the microprobe.

The procedure outlined below was followed, in general, in the preparation of each of the glasses. After weighing, the coarse mixture was stirred slightly, poured into a platinum crucible and fused in a tungsten resistance (Centorr) furnace at 1550° to 1650°C for two to three hours. All mixes were melted at approximately $100\text{--}200^{\circ}\text{C}$ above the melting temperature to decrease viscosity of the liquid and promote mixing. If the mix appeared glassy after the first run, it was cracked out of the crucible into mm size pieces and re-melted under the same conditions; then cracked and melted for a third time. If the mix did not appear glassy after the first run, it was broken and re-melted until it did appear glassy and then melted two more times. Details of preparation of each standard glass are given in Appendix 1.

Analysis of Standards

The ten mixes were analyzed by microprobe at 15KV accelerating potential and 50 nanoamps sample current on brass. Mix C, as an intermediate composition within the volume encompassing the ten mixes in the quaternary system, was the natural choice for a common standard. The data were reduced by the Bence-Albee method using Albee and Ray's correction factors (1970). See Table 1 for a comparison of the weighed-in and analyzed compositions.

The microprobe analyzes a small (on the order of several tens of cubic microns) volume of a polished sample. Since the microprobe analyzes only a small volume of a standard, every volume of the standard must be alike in composition. That is, the standard must satisfy the

criteria of being homogeneous. To check for homogeneity, twenty pieces of each glass (each piece approx 1mm across) were selected at random, mounted and polished for microprobe analysis. Four spots on each piece of glass were analyzed. The glasses were analyzed for homogeneity at 15KV accelerating potential, 50 nanoamps sample current on brass, and an approximately 16 micron fluorescent spot size (measured on anorthite glass). At the beginning of each run, beam current was integrated over a ten second interval. The counting interval for the run was determined by this preset integrated value of beam current. The time (usually about 10 seconds) per counting interval was recorded; the calculated drift never exceeded two percent.

It follows from counting statistics that a frequency distribution of a set of counts (in this case, approx. 80 counts) of a homogeneous sample will follow a Poisson distribution. Consequently, if it can be shown that the variance for any element (set of counts) is strictly due to counting statistics, the glass with respect to that element must be homogeneous. For example, Figure 2 illustrates Poisson distributions calculated for the averages of all elements in Mix B. Intuitively, one might expect that a ratio of the calculated standard deviation (s) to the Poisson standard deviation for the same arithmetic mean (σ) would be quite close to one for a perfectly homogeneous sample. This ratio is commonly termed the "sigma ratio". Sigma ratios were calculated for each element in the ten glasses and are listed in Table 2. Generally, it is accepted that a sigma value less than 1.5 indicates homogeneity.

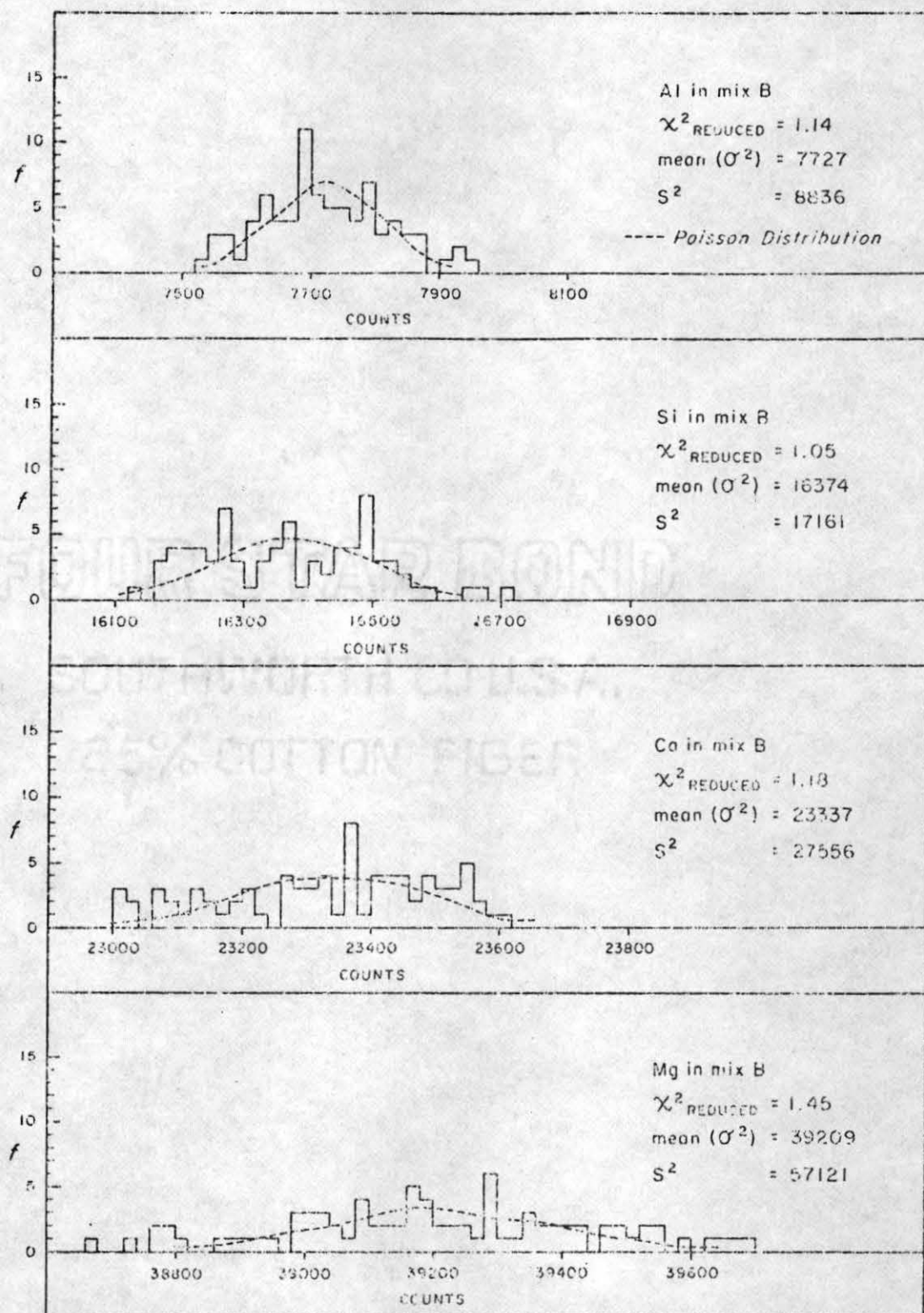


Figure 2. Poisson distributions compared with the observed count distributions for four elements in Mix B.

A more quantitative statement about homogeneity can be obtained using the χ^2 (chi-square) statistic which provides a method of comparing a set of measurements with its supposed parent population when the variance of the measured set (s^2) and the variance of the assumed parent population (σ^2) are known. The ratio, $(s^2)/(\sigma^2) = \chi^2$, is expected to follow the reduced chi-square probability distribution (P) whenever the sample set (s^2) is really a part of the assumed parent (σ^2). A comparison of χ^2 vs. P for various hypothesized levels of inhomogeneity leads to a statement about probable upper limits of inhomogeneity. The approach is most easily explained in terms of an illustrative example.

In Table 2a we present a set of one hundred microprobe analyses taken randomly over a "perfectly homogeneous" sample. To the extent that machine variables can be neglected we would expect the frequency distribution to resemble a Gaussian with $\mu = \bar{N}$ and $\sigma_c^2 = \bar{N}$ (c stands for x-ray "counting"). The histogram shown in Fig. 3a confirms these expectations, i.e., the visual agreement is good. For the set of 100 measurements $s^2 = 10,666$ while for the assumed Gaussian population $\sigma_c^2 = 9,000$ and $\chi^2 = 1.185$. Only one degree of freedom is needed to specify the Gaussian, (\bar{N}), therefore we look up the chi-square probability distribution for $100-1 = 99$ degrees of freedom and find $P = 0.10$, i.e., the chances are 1 in 10 that if our set of 100 counts came from a homogeneous sample with average concentration indicated by \bar{N} , the observed s^2 would be 10,666 or larger. This is a reasonable chance, and we are led to say something like, "it is not at all unlikely that this sample was perfectly homogeneous".

Had we not known "a priori" that the sample was homogeneous we might reasonably have assumed a certain possible level of inhomogeneity, i.e., assumed that the total variance was due to counting statistics plus σ_i^2 , the variance contributed by inhomogeneity. Had we assumed a $\pm 1\%$ level of inhomogeneity:

$$\sigma_i = 0.01(\bar{N}) ; \quad \sigma^2 = 9,000 + ((0.01) (9,000))^2 = 17,100$$

$$\chi^2 = 0.624 ; P > 0.995$$

We are led to conclude that there is very little chance that the sample was as inhomogeneous as $\pm 1\%$. This sets an upper limit on the probable inhomogeneity, but we might well wonder if we have not been too cautious and if the probable upper limits of inhomogeneity have not been set too high. The resolution of that question is to some extent arbitrary and will depend on how conservative we wish to be. For example, it would be quite reasonable to set $P = 0.50$ to obtain the probable limits on inhomogeneity or we could set $P = 0.995$ if we wanted to be very very cautious. In the example we have been considering, these two approaches would yield the following upper limits on inhomogeneity:

$$P = 0.50 ; \quad \chi^2 = 0.993 = 10,666 / (9,000 + \sigma_i^2) ; \quad \sigma_i = 0.46\%$$

$$P = 0.995 ; \quad \chi^2 = 0.672 = 10,660 / (9,000 + \sigma_i^2) ; \quad \sigma_i = 0.92\%$$

We now consider a set of one hundred microprobe analyses taken randomly over a relatively inhomogeneous sample (Table 2b). In Fig. 3b we compare the frequency distribution ($\bar{N} = 9000$ and $s^2 = 248,293$) of this set of measurements with two Gaussian distributions. Both of these

Gaussians have a mean, $\mu = \bar{N} = 9,000$. One Gaussian ($\sigma^2 = \sigma_c^2 = 9,000$) is what we would expect from a perfectly homogeneous sample as in the previous example. It clearly does not correspond to our data set. The other Gaussian ($\sigma^2 = \sigma^2 + \sigma_i^2$, where $\sigma_i = (0.05)(9,000)$) corresponds to what we might expect from an inhomogeneous sample where $\sigma_i = \pm 5.0\%$. In this case the visual agreement is good. Our test should confirm this.

$$P = 0.50; \chi^2 = 0.993 = 248,293 / (9,000 + \sigma_i^2); \sigma_i = 5.46\%$$

$$P = 0.995; \chi^2 = 0.672 = 248,293 / (9,000 + \sigma_i^2); \sigma_i = 6.67\%$$

In Table 2 we list σ_i values (in % for $P = 0.50$) for each of the elements in the synthesized standards. These figures are to be interpreted as reasonable limits to the standard deviation from the average weight concentration for each element.

Table 2. Homogeneity Data for the Ten Glasses

Mix and Element	d.f.	\bar{N}	s^2	Sigma Ratio	σ_i (%)
Mix A					
Si	79	16614	27602	1.23	0.64
Al	79	7989	5170	0.79	"0.00"
Ca	79	25912	32900	1.17	0.33
Mg	79	31259	35177	1.14	0.20
Mix B					
Si	79	16374	17159	1.02	0.19
Al	79	7727	8598	1.07	0.40
Ca	79	23337	26686	1.09	0.26
Mg	79	39209	55344	1.21	0.33
Mix C					
Si	79	17378	10872	0.78	"0.00"
Al	79	6575	4323	0.96	"0.00"
Ca	19*	18023	15917	0.94	"0.00"
Mg	79	47772	57054	1.14	0.22
Mix D					
Si	79	15059	18369	1.08	0.39
Al	79	10346	10704	1.03	0.20
Ca	70	18131	26627	1.19	0.52
Mg	80	53525	71623	1.07	0.26
Mix E					
Si	79	28464	29167	1.08	0.11
Al	79	5013	5654	1.05	0.52
Ca	79	5678	6319	1.06	0.46
Mg	79	17920	32113	1.41	0.67
Mix F					
Si	63	16814	18093	1.01	0.23
Al	67	15989	25565	1.33	0.62
Ca	67	7857	8889	1.11	0.43
Mg	67	30196	58355	1.32	0.56

Table 2. continued

Mix and Element	d.f.	\bar{N}	s^2	Sigma Ratio	σ_i (%)
Mix G					
Si	74	20846	27812	1.16	0.41
Al	75	1520	1118	0.85	"0.00"
Ca	75	3215	4558	1.22	1.16
Mg	74	95882	147094	1.15	0.24
Mix H					
Si	76	9774	9553	1.03	"0.00"
Al	75	21487	22623	1.09	0.17
Ca	75	24840	39490	1.21	0.49
Mg	75	15165	14719	0.95	"0.00"
Mix I					
Si	20*	18090	26507	1.15	0.53
Al	83	967	733	0.87	"0.00"
Ca	20*	28047	63717	1.48	0.69
Mg	83	26494	34395	1.13	0.34
Mix J					
Si	20*	14619	21372	0.96	0.59
Al	84	9615	20801	1.39	1.11
Ca	20*	40117	57937	1.17	0.35
Mg	83	3170	40	0.99	"0.00"

*Glasses I, J and C were analyzed in one experiment; the remaining glasses were analyzed in a second experiment. There appeared to be an analytical problem with the PET crystal on spectrometer one - cause unknown; therefore, these three glasses were re-analyzed during the second experiment (LiF crystal was used instead of PET crystal in the second experiment). Only one spot on each piece of glass (i.e., approx. 20 per mix) was analyzed. A dramatic improvement in the counting statistics for Ca was observed. This improvement was also noticed for Si in Mixes I and J. The counting statistics for Si in C did not change. This improvement was also noticed in subsequent analyses of these three glasses.

Table 2a. One Hundred Replicate Measurements of Counts on One Spot
(or over a Perfectly Homogeneous Specimen). (100 second
counting interval)

No.	Counts	No.	Counts	No.	Counts	No.	Counts
1	8868	26	8805	51	9011	76	8936
2	9000	27	9003	52	8940	77	9066
3	9179	28	8917	53	9050	78	9007
4	9099	29	9160	54	8914	79	8930
5	8995	30	8987	55	9038	80	8965
6	9020	31	9017	56	8875	81	9040
7	8985	32	8926	57	8980	82	8973
8	9055	33	9021	58	9225	83	9107
9	8906	34	8891	59	9079	84	9263
10	9112	35	9125	60	8967	85	8903
11	9028	36	9030	61	8949	86	9057
12	8946	37	8990	62	8979	87	8910
13	9015	38	8969	63	8896	88	9194
14	9090	39	9041	64	9215	89	8867
15	8945	40	8943	65	8875	90	9071
16	9115	41	9096	66	9018	91	8990
17	8818	42	8835	67	8955	92	8997
18	9237	43	9035	68	9065	93	9024
19	8983	44	8887	69	8860	94	9141
20	9070	45	9039	70	9060	95	8975
21	8977	46	8963	71	9100	96	9032
22	9120	47	9078	72	8960	97	8767
23	8922	48	9005	73	9058	98	9043
24	9186	49	8850	74	9083	99	8999
25	8924	50	8720	75	8961	100	9170

Table 2a. continued

<u>Intervals</u>	<u>Prob. x 100</u>	<u>Intervals</u>
9000 - 8981 "+"	(10) 7.93 (7)	9000 "+" - 9019
8981 - 8962	(8) 7.62 (8)	9019 - 9038
8962 - 8943	(6) 7.04 (7)	9038 - 9057
8943 - 8924	(5) 6.24 (6)	9057 - 9076
8924 - 8905	(6) 5.32 (4)	9076 - 9095
8905 - 8886	(4) 4.36 (5)	9095 - 9114
8886 - 8867	(3) 3.43 (3)	9114 - 9133
8867 - 8848	(3) 2.60 (1)	9133 - 9152
8848 - 8829	(1) 1.89 (2)	9152 - 9171
8829 - 8810	(1) 1.32 (2)	9171 - 9190
8810 - 8791	(1) 0.89 (1)	9190 - 9209
8791 - 8772	(0) 0.57 (2)	9209 - 9228
8772 - 8753	(1) 0.36 (1)	9228 - 9247
8753 - 8734	(0) 0.21 (1)	9247 - 9266
8734 - 8715	(1) 0.12 (0)	9266 - 9285

Histogram
 Points of Gaussian
 Histogram

 $\bar{N} = 9000$ $\sigma = 95$ $.2\sigma = 19$

Table 2b. 100 Analysis Points Over an Inhomogeneous Sample
(100 second intervals)

No.	Counts	No.	Counts	No.	Counts	No.	Counts
1	10,312	26	9199	51	9125	76	9457
2	8372	27	8845	52	8537	77	8799
3	9384	28	9357	53	9311	78	9578
4	8759	29	8739	54	8982	79	9732
5	9280	30	9642	55	9475	80	8700
6	7999	31	9072	56	9160	81	9410
7	9780	32	9056	57	7752	82	9187
8	9551	33	8451	58	9220	83	9226
9	7899	34	9131	59	8609	84	7867
10	9065	35	9290	60	8825	85	9370
11	8180	36	8820	61	9998	86	8437
12	9181	37	9300	62	8559	87	9650
13	8476	38	8850	63	8689	88	8976
14	9043	39	10,160	64	9062	89	9588
15	8729	40	9388	65	8127	90	8830
16	9420	41	8923	66	9856	91	8509
17	8302	42	9094	67	8976	92	9497
18	8621	43	8840	68	9100	93	8900
19	9030	44	9088	69	8492	94	8381
20	8808	45	8835	70	8989	95	9255
21	9094	46	9274	71	9707	96	8759
22	8592	47	8800	72	8670	97	9015
23	8722	48	8910	73	8680	98	8259
24	8097	49	8915	74	8709	99	9091
25	9007	50	7950	75	9146	100	9481

Table 2b. continued

<u>Intervals</u>	<u>Prob. x 100</u>	<u>Intervals</u>
9000 - 8908"+"	(7) 7.93 (10)	9000"+"- 9092
8908 - 8816	(8) 7.62 (8)	9092 - 9184
8816 - 8724	(7) 7.04 (6)	9184 - 9276
8724 - 8632	(6) 6.24 (5)	9276 - 9368
8632 - 8540	(4) 5.32 (6)	9368 - 9460
8540 - 8448	(5) 4.36 (4)	9460 - 9552
8448 - 8356	(6) 3.43 (3)	9552 - 9644
8356 - 8264	(1) 2.60 (3)	9644 - 9736
8264 - 8172	(2) 1.89 (1)	9736 - 9828
8172 - 8080	(2) 1.32 (1)	9828 - 9920
8080 - 7988	(1) 0.89 (1)	9920 - 10012
7988 - 7896	(2) 0.57 (0)	10012 - 10104
7896 - 7804	(1) 0.36 (1)	10104 - 10196
7804 - 7712	(1) 0.21 (0)	10196 - 10288
7712 - 7620	(0) 0.12 (1)	10288 - 10380

Histogram	Gaussian	Histogram

$$\bar{N} = 9000; \sigma^2 = 9000 + \sigma_i^2 = 9000 + 202,500 = 211,500$$

$$\sigma = 460; \sigma_{pp} = 95; \sigma_i = 450 \text{ (5\% inhomogeneity); } .2\sigma = 92.$$

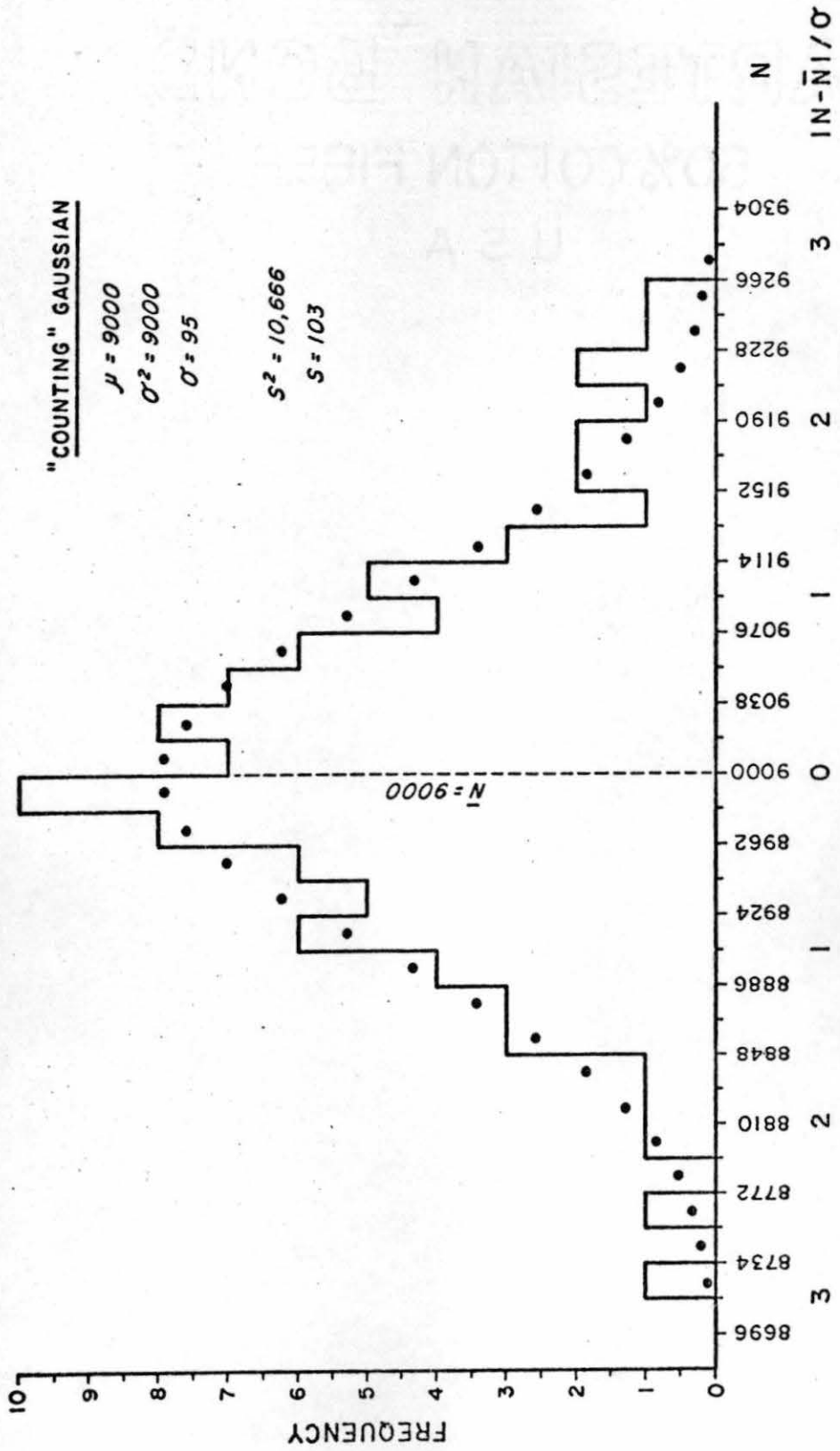


Figure 3a. Histogram of Data taken over "Perfectly Homogeneous Sample".

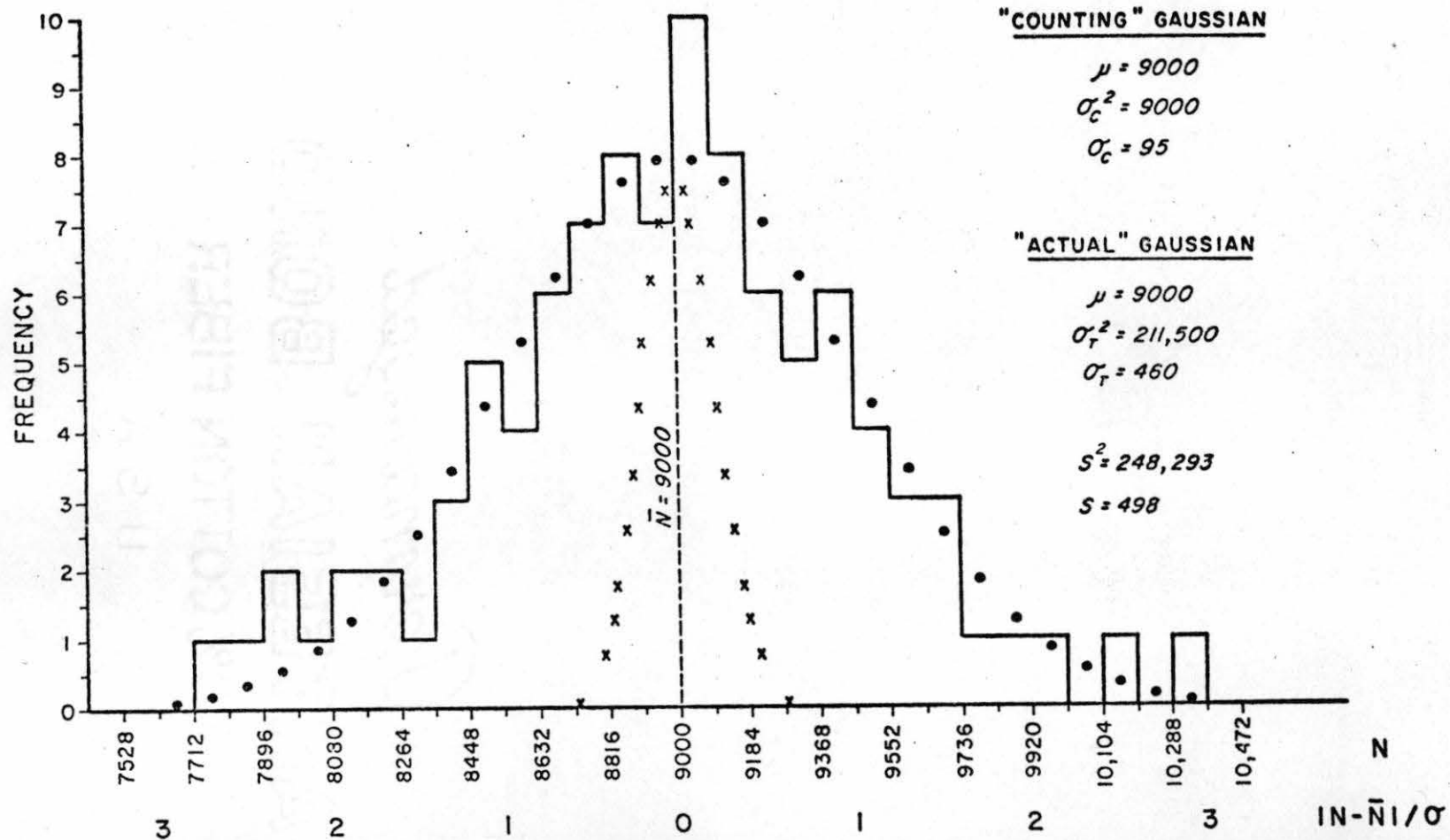


Figure 3b. Histogram of Data taken over "Inhomogeneous Sample".

CORRECTION TECHNIQUES FOR MICROPROBE DATA REDUCTION

There are two approaches to reducing raw microprobe data. Both methods involve multiplying the intensity ratio by a correction factor to obtain the concentration ratio:

$$(1) \quad C_U^n / C_S^n = (k_U^n / k_S^n) \times f.$$

The difference between the two approaches is the way in which f is obtained. The "ZAF" technique uses theoretically derived equations to produce f and the empirical methods use empirically derived correction factors or calibration curves.

ZAF Correction Technique

The ZAF technique corrects for three types of effects: the atomic number effect (Z), the absorption effect (A), and the secondary fluorescence effect (F). The product of these three factors is the total correction factor, T. The set of equations as recommended by Yakowitz (1975) was employed in this project.

The atomic number effect depends upon two quantities - the electron stopping power and the electron backscattering. Electron backscattering occurs when an incident electron is elastically deflected (scattered) in passing close to an atomic nucleus. The electron leaves the sample without generating X-rays. The backscatter factor is dependent upon the

critical excitation potential of the element being analyzed, the accelerating potential, the atomic number of each element in the matrix, and the weight fraction of each element. There is a given probability of ionization (and subsequent X-ray generation) by an electron traveling a given distance through the sample. This probability is roughly proportional to the distance the electron travels in a material before its energy falls below the critical excitation level of the element being analyzed. This distance is determined by the stopping power of a sample. The stopping power factor is dependent upon the critical excitation energy of the analyzed element, accelerating potential, atomic number of each of the matrix elements in the sample, atomic weight of those elements and their weight fractions in the sample. The quotient of the stopping power and the electron backscattering quantities (stopping power/backscattering) equals the atomic number correction (Z).

The second correction is the absorption correction (A). Due to absorption, the intensity of electron excited X-rays emerging from the sample is less than the intensity produced by incident electrons. Incident electrons penetrate a sample and generate characteristic X-rays below the surface of the sample. As X-rays pass through the sample, some of the X-ray photon energy is expended in the ionization of inner atomic shells and in other processes. The amount of absorption of energy depends upon the thickness through which the X-ray travels and the mass absorption coefficient of the sample. The total absorption is integrated over an infinite volume. This integral depends on the mass

absorption coefficient, the cosecant of the take-off angle (the angle between the sample surface and the X-ray path to the spectrometer) and the distribution of X-ray production with depth in the sample. This distribution depends upon the average atomic number, the atomic weights of the constituent elements, accelerating potential and the critical excitation potential of the analyzed element.

The third correction is for secondary fluorescence (F). Incident electrons may excite characteristic X-rays that are higher in energy than the absorption edge of the element being analyzed. These energetic X-rays may excite X-rays characteristic of the element being analyzed. The X-ray intensity produced by that element is increased and the apparent concentration of that element is increased. The magnitude of the fluorescence correction is calculated via a complex equation depending primarily on the weight concentrations of the exciting elements in the matrix and the fluorescent yields of those elements. Fluorescence also depends upon atomic number, accelerating potential, atomic weight, critical excitation potential of the analyzed element and the mass absorption coefficients for the matrix elements.

The three corrections - Z, A and F - are made for the standard and for the unknown. Since the concentrations of the elements in the unknown are not known, these concentrations are first approximated by the X-ray intensities measured by the microprobe. The elemental composition of the unknown is calculated using the resulting correction factors. For element n in an unknown:

$$(1a) \quad C_u^n / C_s^n = (k_u^n / k_s^n) \times ((Z_u X_A X_F)_u / (Z_s X_A X_F)_s).$$

This second estimate of the concentration of element n in the unknown is used to re-calculate the correction factor for the unknown. This process is repeated for each element in the unknown until the results converge. The ZAF correction process (abstracted from a program written for a 9830 Hewlett Packard computer) is shown in detail in Appendix 2 using a pure element standard. Whether done by hand or by computer, this method can be complex and time consuming for multicomponent systems.

Empirical Correction Techniques

There are two empirical approaches to data reduction, calibration curves and the use of empirical correlation coefficients. The calibration curve method involves a series of standards close in composition to the unknown to be analyzed. X-ray intensities of the elements of interest are measured for each standard. Curves of X-ray intensity versus elemental weight concentrations are plotted and the unknown concentrations are determined from these curves. When dealing with complex silicates, this method can become extremely complicated due to the potentially large number of independently variable concentrations. The second empirical approach employs the empirical correction factor or "correlation coefficient". These coefficients may be produced by the solution of a series of linear equations and applied to a wide variety of compositions.

Empirical correlation coefficients have been used to reduce X-ray fluorescence data since the mid-1950's. Ziebold and Ogilvie (1964)

developed an empirical equation for the calculation of chemical compositions from probe analyses. Using binary metal alloys, they found that the plots of concentration/intensity versus concentration of an element were almost linear (the straight line fit was within the variance of the individual points). They produced the straight line function:

$$(2) \quad C_{ab}^a \div (k_{ab}^a/k_a^a) = \alpha_{ab}^a + (1-\alpha_{ab}^a) \times C_{ab}^a$$

where C_{ab}^a equals the ratio of the weight fraction of element a in the binary alloy ab to the weight fraction of element a in pure a; k_{ab}^a/k_a^a equals the ratio of the X-ray intensity of a characteristic line produced by element a in the alloy to that intensity produced by element a in the pure material and α is the limit of $C_{ab}^a \div (k_{ab}^a/k_a^a)$ as C_{ab}^a approaches zero. The superscript a and the subscript ab indicate element a in binary mix ab respectively. α_{ab}^a is a measure of the effect of element b in the binary mix upon the X-ray intensity produced by a. This correction factor may be related to the theoretical correction factor. If $\alpha > 1$, then absorption is important. If $\alpha < 1$, then secondary fluorescence is important. There is no theoretical basis for this approach; the equation merely fits the observed data.

Ziebold and Ogilvie (1964) extended this empirical approach to multicomponent systems. Suppose one has determined α_{ab}^a and α_{ac}^a in the respective binary systems. Consider a ternary system, abc. Extending Equation (2) for the ternary case:

$$(3) \quad C_{abc}^a \div (k_{abc}^a/k_a^a) = \bar{\alpha}_{abc}^a + (1-\bar{\alpha}_{abc}^a) \times C_{abc}^a$$

where

$$(4) \quad \bar{\alpha}_{abc}^a = (\alpha_{ab}^a \times C_{abc}^b + \alpha_{ac}^a \times C_{abc}^c) / (C_{abc}^b + C_{abc}^c).$$

The ternary correlation coefficient is the weighted average of the binary correlation coefficients.

Bence and Albee (1968) extended the correlation coefficient as suggested by Ziebold and Ogilvie to the use of oxide rather than element components and then to multicomponent oxide systems. Equations (2), (3) and (4) are applied to oxide systems by the following: C_{nm}^n becomes the weight concentration of the oxide of n in the oxide system $nO+mO$; α_{nm}^n becomes the effect of oxide m in the oxide system $nO+mO$ upon the intensity of characteristic X-rays produced by element n; k_n^n becomes the intensity of characteristic X-rays produced by element n in the pure oxide of n; and k_{nm}^n becomes the intensity of characteristic X-rays produced by element n in $nO+mO$.

Calculation of Alpha Factors

Bence and Albee (1968), and Albee and Ray (1970) have determined alpha factors for many oxide pairs. In a few instances, the alpha factors were determined directly by measuring X-ray intensities in binary oxide systems and calculating alpha factors from Equation (2). Many of these alpha factors, however, were indirectly determined. They were calculated using the theoretical correction factor approach mentioned previously. For such cases, the so-called empirical correction factor approach is merely a mathematical approximation of the

theoretical approach. That is, theoretically derived binary alpha factors are linearly combined to produce an "empirical" correction factor. These factors are not independent of the many approximations and simplifications inherent in the theoretical method. Obviously, it is desirable to empirically produce a set of alpha factors independent of the complex theoretical formulae.

A set of alpha factors may be simply calculated from empirical data. Re-arranging Equation (3) (all of the following are for oxides):

$$(3) \quad C_u^a \div (k_u^a/k_a^a) = (\bar{\alpha}_{au}^a \times (1-C_u^a)) + C_u^a$$

where $\bar{\alpha}_{au}^a$ is the same as $\bar{\alpha}_{abc}^a$ except u represents any multicomponent oxide system including aO. $\bar{\alpha}_{au}^a$ is the weighted average of the individual alpha factors excluding the factor α_{aa}^a :

$$(5) \quad \bar{\alpha}_{au}^a = \frac{\sum_{n \neq a} (C_u^n \times \alpha_{an}^a)}{(1-C_u^a)}$$

Combining Equations (3) and (5):

$$(6) \quad C_u^a \div (k_u^a/k_a^a) = (\alpha_{ab}^a \times C_u^b + \alpha_{ac}^a \times C_u^c + \dots + \alpha_{an}^a \times C_u^n) + C_u^a$$

α_{aa}^a is defined as being equivalent to one so it may be included in Equation (6):

$$(7) \quad C_u^a \div (k_u^a/k_a^a) = \alpha_{aa}^a \times C_u^a + \alpha_{ab}^a \times C_u^b + \alpha_{ac}^a \times C_u^c + \dots + \alpha_{an}^a \times C_u^n$$

The summation on the right hand side of Equation (7) is equivalent to beta (β , see Bence and Albee, 1968). Notice that beta is not equivalent to $\bar{\alpha}_{au}^a$. Consider, for example, a quaternary oxide system with oxides 1, 2, 3 and 4; element 1 is being analyzed:

$$(8) \quad C_u^1 \div (k_u^1/k_l^1) = \sum_{i=1}^4 (\alpha_{li}^1 \times C_u^i) = \beta.$$

For a glass of known composition, C_u^1 , C_u^2 , C_u^3 and C_u^4 are known and given the pure oxide of 1, (k_u^1/k_l^1) may be measured. Since α_{11}^1 is equivalent to one, there are three unknowns in this equation. Given at least three different glasses within this system, the set of resulting equations may be solved for the three alpha factors. This four component system includes 16 alpha factors, four of which are equal to one. Therefore, a total of twelve alpha factors can be produced given three glasses and the four oxides within a four component system. If more than three glasses are used, the alpha factors may be calculated using the linear regression method or a least squares fit.

The four component oxide system within which the glass standards were produced closely approximates the compositions of many rocks and minerals. Therefore, alpha factors involving the interrelationships of SiO_2 , Al_2O_3 , CaO and MgO are useful to geologists in the reduction of microprobe data. The second section of this project was devoted to the calculation of the twelve alpha factors within this system.

The first requirement in calculating the twelve alpha factors was to have three or more homogeneous mixes of well known composition from which the Si, Al, Ca and Mg X-ray intensities could be measured. The second was to have the end member oxides in a form that could also be analyzed by the microprobe. The ratio:

$$I_u^a = k_u^a/k_a^a$$

where k_u^a equals the characteristic X-ray intensity produced by element

a in a mix and k_a^a equals the intensity produced by element a in the pure oxide of a, could then be measured and with the compositions of the mixes be used to form a series of equations:

$$\begin{aligned} C_1^a/I_1^a &= \alpha_{aa}^a C_1^a + \alpha_{ab}^a C_1^b + \alpha_{ac}^a C_1^c + \alpha_{ad}^a C_1^d \\ C_2^a/I_2^a &= \alpha_{aa}^a C_2^a + \alpha_{ab}^a C_2^b + \alpha_{ac}^a C_2^c + \alpha_{ad}^a C_2^d \\ C_3^a/I_3^a &= \alpha_{aa}^a C_3^a + \alpha_{ab}^a C_3^b + \alpha_{ac}^a C_3^c + \alpha_{ad}^a C_3^d \\ &\vdots \quad \quad \quad \vdots \quad \quad \quad \vdots \quad \quad \quad \vdots \quad \quad \quad \vdots \end{aligned}$$

where each equation represents a different mix (numbered subscripts; see Appendix 3) and the letters stand for the four elements (or oxides). The last requirement was to have a method of solving the set of linear equations.

Experimental Procedure

The ten standard glasses produced for the first half of this project filled the first requirement. They had been proven homogeneous, their compositions were known more exactly than could be analyzed by the probe. Two pieces of each glass, about two-three mm across, were mounted in one polished section and analyzed. The natural quartz, synthetic periclase and synthetic alumina used as starting materials for the glasses were used to obtain k_n^n values. The synthetic, crystalline CaO presented a problem in mounting, polishing and analyzing. CaO is unstable in the air. It reacts with H_2O to form $Ca(OH)_2$ and with CO_2 to form $CaCO_3$. The CaO could have become contaminated to an unknown

degree during polishing and handling. Also, the stability of CaO under the electron beam was poorly known. Therefore, an indirect method of obtaining k_{CaO}^{Ca} was followed. Synthetic CaF_2 and natural calcite (clear Iceland Spar obtained from the University of Oregon, Geology Department mineral collection) were mounted with a piece of the CaO. The surfaces of the crystals were sealed in epoxy until polishing. All the polishing was done under oil. The mount was cleaned between polishing steps in xylene and transferred to the carbon coater immediately upon completion of polishing and placed under a vacuum until analysis. A piece of the CaF_2 and the $CaCO_3$ were also included in the mount with the MgO and quartz (Al_2O_3 mounted separately due to extreme hardness). The CaO, CaF_2 and $CaCO_3$ were analyzed at 15KV accelerating potential and 50 nanoamps sample current on brass. The ratios - $k_{CaF_2}^{Ca}/k_{CaO}^{Ca}$ and $k_{CaCO_3}^{Ca}/k_{CaO}^{Ca}$ - were measured. These ratios are not quite equal to the ratios - $C_{CaF_2}^{Ca}/C_{CaO}^{Ca}$ and $C_{CaCO_3}^{Ca}/C_{CaO}^{Ca}$ - respectively. The Bence-Albee method predicts a small correction, β ($\beta \times "k" \text{ ratio} = "C" \text{ ratio}$). This correction is 0.971 for Ca in CaF_2 and 1.004 for Ca in $CaCO_3$. The theoretical method (Appendix 2) produces small but different corrections - 0.998 for Ca in CaF_2 and 1.051 for Ca in $CaCO_3$. None of these corrections are the same as the empirical corrections produced by the experiment outlined above. The values of the concentration ratios and the observed intensity ratios are:

$$C_{CaF_2}^{Ca}/C_{CaO}^{Ca} = 0.718$$

$$k_{CaF_2}^{Ca}/k_{CaO}^{Ca} = 0.741$$

$$C_{CaCO_3}^{Ca}/C_{CaO}^{Ca} = 0.560$$

$$k_{CaCO_3}^{Ca}/k_{CaO}^{Ca} = 0.537$$

That is, these empirically produced corrections are 0.969 for Ca in CaF_2 and 1.043 for Ca in CaCO_3 . Both the Bence-Albee method (using theoretically derived α factors) and the theoretical method are based on theoretical equations. The purpose of this exercise was to produce empirical correction factors. Incorporating a theoretical factor in the calculations would defeat that purpose. Therefore, the empirically produced intensity ratios were adopted and used to calculate $k_{\text{CaO}}^{\text{Ca}}$ for each alpha factor run (see Appendix 4 for a further discussion of the intensity ratios). The X-ray intensities produced by Ca in CaCO_3 and CaF_2 were measured and with the adopted "k" ratios, two values of $k_{\text{CaO}}^{\text{Ca}}$ were calculated (the two values differed by 2% of the average). Each of these values was given equal weight; the average was used in the calculation of alpha factors.

The procedure outlined below was followed during each microprobe run used to collect data for alpha factor calculations. Before each run, both the standard mounts and oxide mounts were re-polished; then carbon coated together. The microprobe was allowed to "warm up" for one and a half to two hours. Calcium ($K\alpha$ radiation for all elements, for all runs) was analyzed using an LiF crystal, aluminum and silicon were analyzed using an ADP crystal, and magnesium was analyzed using an RAP crystal. Sample current was set at 50 nanoamps on brass. The fluorescent spot size was set at approximately 20 microns on anorthite glass before starting each run. All analyses were done at a preset integrated value of beam current chosen so that counts were accumulated over approximately a ten second interval. The time was recorded during

each counting interval and less than two percent drift (in time) was observed during each run. Backgrounds for calcium, magnesium and silicon were measured (on peak) on the alumina; background counts for aluminum were taken on quartz. At the beginning of each cycle, counts were taken ten times on each oxide and backgrounds were repeated four times on the alumina and/or quartz. Ten areas of each glass (five spots on each of two pieces) were analyzed for each standard mix. At the end of each cycle the oxide analyses and backgrounds were repeated. A run consisted of two cycles - calcium, magnesium and aluminum or silicon were analyzed during the first cycle and aluminum or silicon was analyzed during the second cycle. An entire run including peaking in of the spectrometers took under four hours. This procedure was followed so that differences between the analysis conditions of each glass (in fact, each spot) would be minimized.

The means of each set of counts were corrected for background. The oxide count averages were calculated at the beginning of a cycle and the end of a cycle and compared. If the difference between the averages was greater than one standard deviation, the oxide counts were corrected for drift in the following manner: the drift was assumed to be linear and one tenth (an increment for each of the ten glasses) of the difference was successively added (or subtracted) to the initial average oxide count, and paired with the appropriate glass according to its order of analysis (the glasses were always analyzed in alphabetical order). The initial oxide average was paired with the first analyzed glass. Drift was rarely encountered and the few examples of

drift encountered are listed in Appendix 4. Drift during the analysis of any single glass was not observed. If the number of counts per second exceeded 10,000, the following deadtime correction was made:

$$(9) \quad N = ((N_o/10)/(1-(N_o \times \tau/10))) \times 10$$

where N_o equals the counts observed, N equals the "true" number of counts and τ for each of the three spectrometers was $2-3 \times 10^{-6}$ sec. A deadtime correction was made primarily on oxide counts at 30KV accelerating potential (see Appendix 4).

The corrected counts and the known compositions in weight fraction of the glasses were arranged in Equation (8). This equation was modified to:

$$(8a) \quad (C_1^n / (k_1^n / k_n^n)) - C_1^n = \sum_{i=1}^n C_1^i \alpha_{ni}$$

The difference on the left hand side of the equation and the C_1^i 's for each glass were input in a linear least squares program. Appendix 3 lists the data just as it was input in the least squares program. Forty sets of {difference, C_1^i } were produced for the ten glasses at each accelerating potential. That is, ten equations were available to solve for the three alpha factors of each of the four elements - Ca, Mg, Si and Al.

Since theoretical correction factors vary with accelerating potential, one would expect empirical correction factors to vary in a similar fashion. A difference in theoretically derived alpha factors at 15KV and 20KV has been shown by Albee and Ray (1970). A variation with take-off angle was also shown by Albee and Ray (1970). All alpha

factors calculated for this project are for an angle of 52.5° . The procedure for empirically deriving alpha factors was repeated for runs at 10KV, 15KV, 20KV and 30KV accelerating potentials. The ratios used to calculate $k_{\text{CaO}}^{\text{Ca}}$ at 15KV were used at all four accelerating potentials.

Theoretical Alpha Factor Calculation

The alpha factor may be calculated from the theoretical correction factor, T. Appendix 2 abstracts the method used to calculate T using a pure element standard. Using this method, T for an element in a mix and T for an element in the oxide must be calculated in order to solve the empirical equation (for oxides):

$$(8) \quad (C_{\text{mix}}^n / C_{\text{no}}^n) \div (k_{\text{mix}}^n / k_{\text{no}}^n) = \beta$$

for beta and ultimately for alpha:

$$(8) \quad \beta = \sum_i C_i^1 \alpha_{ni}^n.$$

The following method (abstracted from a subroutine of the 9830 program mentioned in the section, "ZAF Correction Technique") was used to theoretically calculate beta and alpha. Consider the simple binary oxide system - $\text{MgO} + \text{SiO}_2$, analyzing for Mg. All C's represent weight fractions of an element or oxide (noted). The concentrations $C_{\text{mix}}^{\text{MgO}}$, $C_{\text{mix}}^{\text{Mg}}$, $C_{\text{mix}}^{\text{O}}$ and $C_{\text{mix}}^{\text{SiO}_2}$ are known.

$$(1a) \quad C_{\text{mix}}^{\text{Mg}} / C_{\text{Mg-metal}}^{\text{Mg}} = (k_{\text{mix}}^{\text{Mg}} / k_{\text{Mg-metal}}^{\text{Mg}}) \times T$$

Since $C_{\text{Mg-metal}}^{\text{Mg}} \equiv 1$, it will be omitted from the following equations.

$$(8) \quad (C_{\text{mix}}^{\text{MgO}} / C_{\text{MgO}}^{\text{MgO}}) \div (k_{\text{mix}}^{\text{Mg}} / k_{\text{MgO}}^{\text{Mg}}) = C_{\text{mix}}^{\text{MgO}} \alpha_{\text{Mg-MgO}}^{\text{Mg}} + C_{\text{mix}}^{\text{SiO}_2} \alpha_{\text{Mg-SiO}_2}^{\text{Mg}}$$

The right hand sum, of course, equals β and $C_{MgO}^{MgO} = 1$. Notice that k_{MgO}^{Mg} appears in Equation (8) and not in Equation (1a). This necessitates the calculation of T for Mg in MgO (T_o):

$$(1a) \quad C_{MgO}^{Mg} = (k_{MgO}^{Mg} / k_{Mg-metal}^{Mg}) \times T_o.$$

These three equations may be combined to solve for beta (β):

$$(10) \quad \beta = (C_{mix}^{MgO} \times C_{MgO}^{Mg} \times T) / (T_o \times C_{mix}^{Mg}).$$

In this binary system:

$$(\beta - C_{mix}^{MgO}) / C_{mix}^{SiO_2} = \alpha_{Mg-SiO_2}^{Mg}.$$

If the mix is composed of more than two oxides,

$$\beta - C_{mix}^n = \sum_{i \neq n} C_{mix}^i \alpha_{ni}^n$$

where C stands for oxide weight fraction and the set of such linear equations may be solved for the alpha factors as were the sets of empirical linear equations by the linear least squares method (see Appendix 3 for data involved in these calculations).

Using the theoretical procedure outlined previously and in Appendix 2, alpha factors were calculated for all the binary systems within the four component oxide system studied. Alpha factors were calculated at ten mole percent intervals in each binary system. Alpha factor values versus weight fraction oxide are plotted in Figures 4-9. Alpha factors are considered to be constant, i.e., they are used as if independent of composition. Tables 3 and 4 list the alpha factors calculated by the empirical method ($E\alpha$), the theoretical alpha factors calculated from the binary mixes ($B\alpha$), the theoretical alpha factors calculated by the

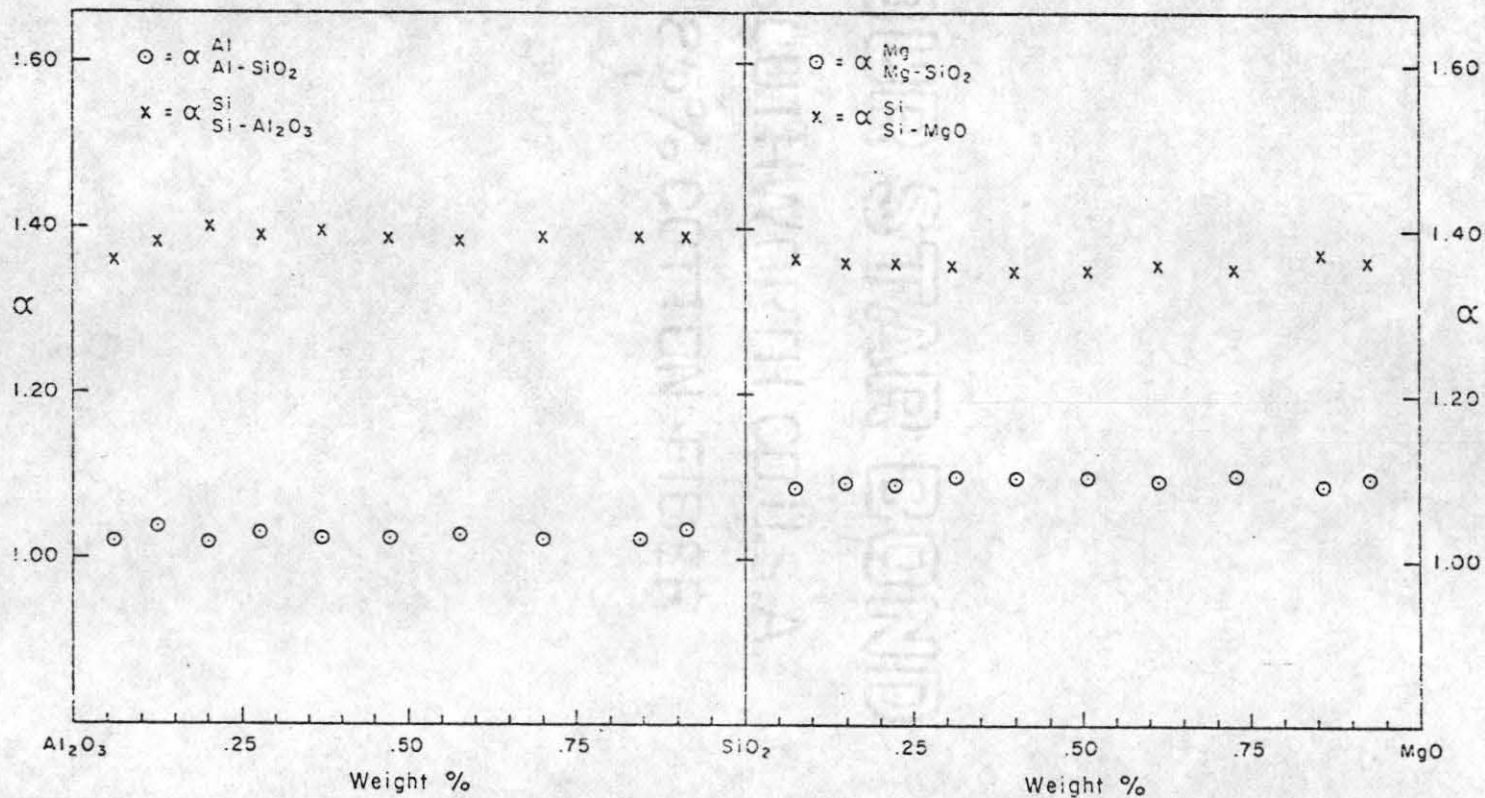


Figure 4. Theoretical binary alpha factors involving Al_2O_3 and SiO_2 .

Figure 5. Theoretical binary alpha factors involving SiO_2 and MgO .

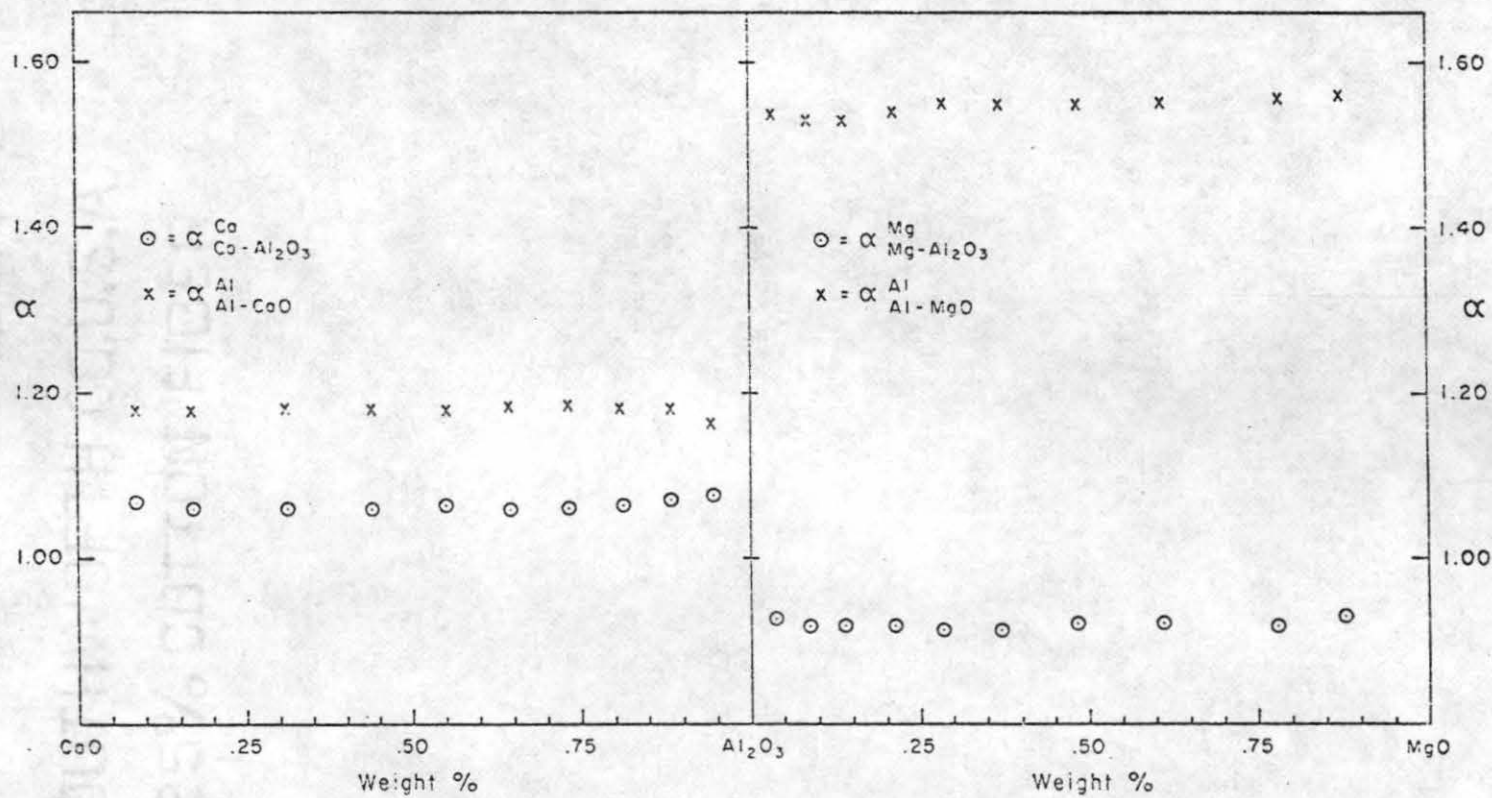


Figure 6. Theoretical binary alpha factors involving CaO and Al_2O_3 .

Figure 7. Theoretical binary alpha factors involving Al_2O_3 and MgO .

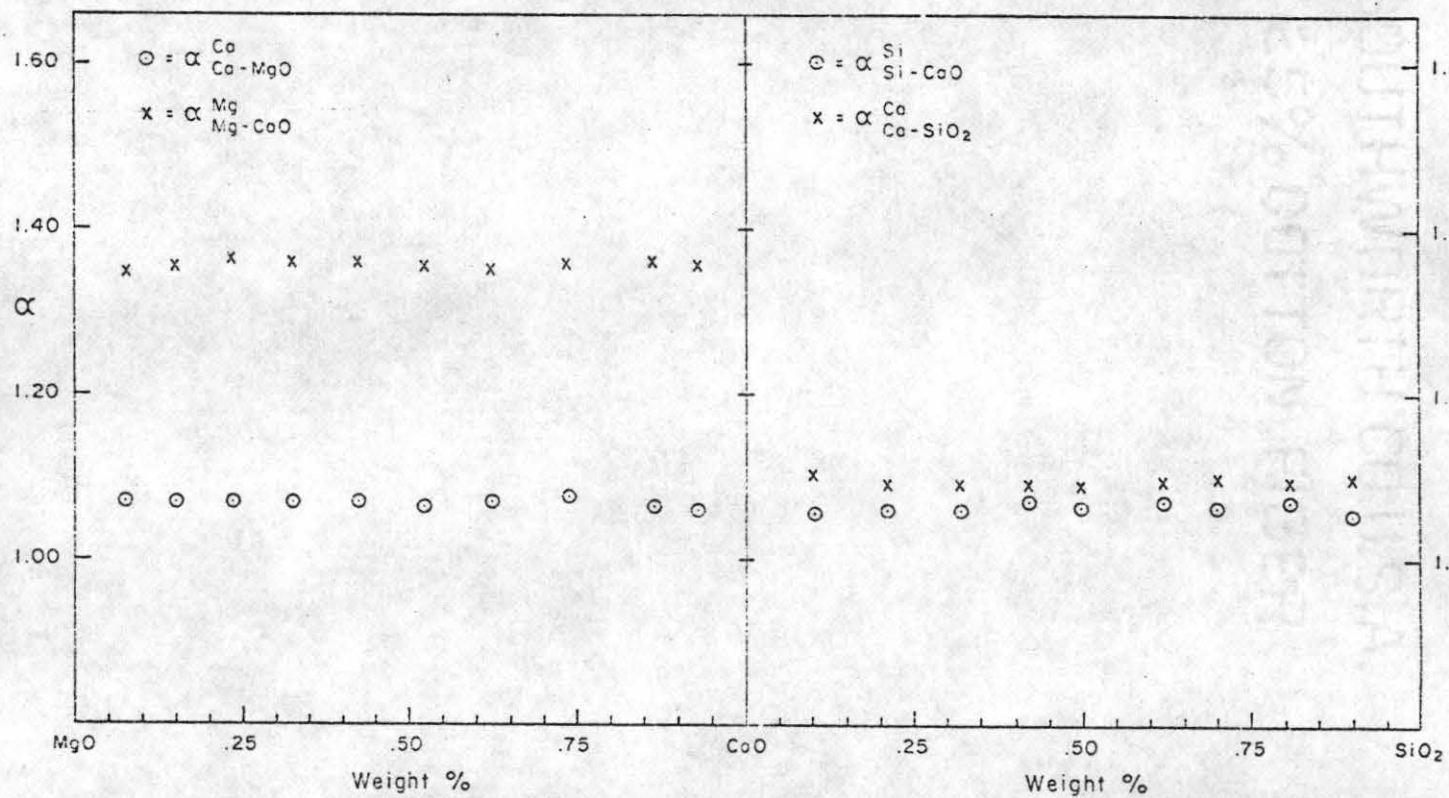


Figure 8. Theoretical binary alpha factors involving MgO and CaO.

Figure 9. Theoretical binary alpha factors involving CaO and SiO₂.

least squares method from the ten mixes ($T\alpha$), the Bence and Albee alpha factors ($B-A\alpha$), and the Albee and Ray alpha factors ($A-R\alpha$). Included in these tables are the errors propagated by the linear least squares method (LLSQ errors).

Uncertainties in Alpha Factors

Uncertainties exist in the calculation of the alpha factors by any of the methods employed in this project. Figures 4-9 graphically show the scatter (uncertainty) in alpha factors calculated theoretically for binary systems. Given the uncertainty in the input data, the error propagated by the least squares method may be calculated (Young, 1962; p.105 and pp.98-99). For a given set of equations (group of mixes), the error propagated by each equation may be calculated. The total error associated with an alpha factor is the average of these errors propagated by each equation. Appendix 3 gives the errors propagated by each equation for $T\alpha$'s and $E\alpha$'s. Tables 3 and 4 list the averages of these errors. It should be noted that the errors in $T\alpha$ are consistently negligible because there is no uncertainty in the input data (some uncertainty, if the weighing error in mix composition is included). The following discussion deals, therefore, with the errors propagated by the least squares method for empirical alpha factors only.

The largest errors are associated with alpha factors in which MgO is the "affecting" oxide. The individual errors propagated by each equation were studied (Appendix 3) and it was observed that one glass contributed the greatest error to each alpha factor of the form α_{n-MgO}^n .

Table 3. Alpha Factors Calculated by Several Methods at 15 KV

α Factor	A-R α	B-A α	B α	T α	LLSQ Error	E α	LLSQ Error
$\alpha_{\text{Si-Al}_2\text{O}_3}^{\text{Si}}$	1.43	1.34	1.39	1.37	$\pm 1 \times 10^{-6}$	1.34	$\pm .03$
$\alpha_{\text{Si-CaO}}^{\text{Si}}$	1.05	1.03	1.06	1.09	$< 1 \times 10^{-6}$	0.98	$\pm .03$
$\alpha_{\text{Si-MgO}}^{\text{Si}}$	1.39	1.29	1.36	1.37	$\pm 1.8 \times 10^{-5}$	1.30	$\pm .13$
$\alpha_{\text{Al-SiO}_2}^{\text{Al}}$	1.04	1.01	1.03	1.04	$< 1 \times 10^{-6}$	0.81	$\pm .003$
$\alpha_{\text{Al-CaO}}^{\text{Al}}$	1.14	1.18	1.18	1.30	$\pm 1 \times 10^{-6}$	0.90	$\pm .11$
$\alpha_{\text{Al-MgO}}^{\text{Al}}$	1.62	1.62	1.55	1.29	$\pm 3.7 \times 10^{-5}$	1.48	$\pm .80$
$\alpha_{\text{Ca-SiO}_2}^{\text{Ca}}$	1.08	1.18	1.09	1.07	$< 1 \times 10^{-6}$	1.10	$\pm .0007$
$\alpha_{\text{Ca-Al}_2\text{O}_3}^{\text{Ca}}$	1.06	1.11	1.06	1.10	$\pm 2 \times 10^{-6}$	1.07	$\pm .06$
$\alpha_{\text{Ca-MgO}}^{\text{Ca}}$	1.08	1.10	1.07	1.06	$\pm 1.8 \times 10^{-5}$	1.01	$\pm .11$
$\alpha_{\text{Mg-SiO}_2}^{\text{Mg}}$	1.09	1.16	1.10	1.10	$< 1 \times 10^{-6}$	1.17	$\pm .0004$
$\alpha_{\text{Mg-Al}_2\text{O}_3}^{\text{Mg}}$	1.03	1.02	1.02	1.00	$\pm 3 \times 10^{-6}$	1.09	$\pm .02$
$\alpha_{\text{Mg-CaO}}^{\text{Mg}}$	1.26	1.20	1.36	1.36	$\pm 2 \times 10^{-6}$	1.36	$\pm .01$

Table 4. $T\alpha$ and $E\alpha$ Factors Calculated at 10 KV, 20 KV, 30 KV.

α Factor	10 KV		20 KV			30 KV	
	$T\alpha^*$	$E\alpha$	$T\alpha$	$E\alpha$	A-R α	$T\alpha$	$E\alpha$
α_{Si}^{Si} $\alpha_{Si-Al_2O_3}^{Si}$	1.18	1.16 \pm .06	1.56	1.60 \pm .04	1.67	1.88	2.23 \pm .04
α_{Si}^{Si} α_{Si-CaO}^{Si}	1.04	0.99 \pm .04	1.18	0.94 \pm .03	1.10	2.86	1.18 \pm .03
α_{Si}^{Si} α_{Si-MgO}^{Si}	1.20	1.14 \pm .25	1.54	1.45 \pm .27	1.58	1.66	2.05 \pm .20
α_{Al}^{Al} $\alpha_{Al-SiO_2}^{Al}$	1.01	0.96 \pm .003	1.03	0.97 \pm .002	1.05	1.02	1.02 \pm .002
α_{Al}^{Al} α_{Al-CaO}^{Al}	1.10	1.11 \pm .39	1.40	1.25 \pm .19	1.22	—	1.52 \pm .29
α_{Al}^{Al} α_{Al-MgO}^{Al}	1.35	1.41 —	1.83	2.03 —	1.92	2.10	2.72 \pm .25
α_{Ca}^{Ca} $\alpha_{Ca-SiO_2}^{Ca}$	1.05	1.08 \pm .002	1.10	1.15 \pm .0005	1.12	1.18	1.22 \pm .001
α_{Ca}^{Ca} $\alpha_{Ca-Al_2O_3}^{Ca}$	1.08	1.01 \pm .29	1.12	1.12 \pm .04	1.09	1.19	1.19 \pm .04
α_{Ca}^{Ca} α_{Ca-MgO}^{Ca}	1.05	0.99 \pm .27	1.08	1.07 \pm .06	1.09	1.13	1.07 \pm .06
α_{Mg}^{Mg} $\alpha_{Mg-SiO_2}^{Mg}$	1.06	1.15 \pm .0008	1.16	1.20 \pm .0005	1.15	1.15	1.26 \pm .0004
α_{Mg}^{Mg} $\alpha_{Mg-Al_2O_3}^{Mg}$	0.98	1.09 \pm .02	0.99	1.10 \pm .03	1.06	1.02	1.14 \pm .02
α_{Mg}^{Mg} α_{Mg-CaO}^{Mg}	1.16	1.17 \pm .02	2.13	1.55 \pm .01	1.40	—	1.72 \pm .01

*LLSQ errors are not included—they are negligible, see Appendix 3.

This glass, Mix J, contains only one percent MgO - the lowest concentration of any one oxide in any of the ten mixes. This is understandable since an oxide of very small concentration contributes a small correction regardless of the value of the alpha factor in the reduction of raw data ($1/C^2$ is a factor in the error propagation equation). Therefore, the alpha factors of the form α_{n-MO}^n predicted by a mix with a very small concentration of oxide MO are not significant. To attach a more realistic error to the alpha factors (at 15KV only), groups of nine mixes were used to calculate $E\alpha$. The values of these alpha factors were not different from those calculated using ten mixes. However, the errors propagated by the least squares method were greatly reduced by eliminating mixes of the type described above. Table 5 shows these "improved" errors along with the mixes eliminated in their calculation.

Variation in Values of Alpha Factors

The values of alpha factors appear to be dependent upon the compositions of the mixes used to calculate the alpha factors. The more equations used to calculate an alpha factor, the less important an individual mix becomes. To study the effects of individual mixes upon the calculation of alpha factors, all possible groups of three out of the ten mixes were used to give exact solutions to the linear equations by the least squares method. Both theoretical and empirical alpha factors were calculated for a 15KV accelerating potential. The results of these calculations were a set of 120 theoretical and 120 empirical values for each of the twelve alpha factors. These results are shown

FOUR-STAR-BOND

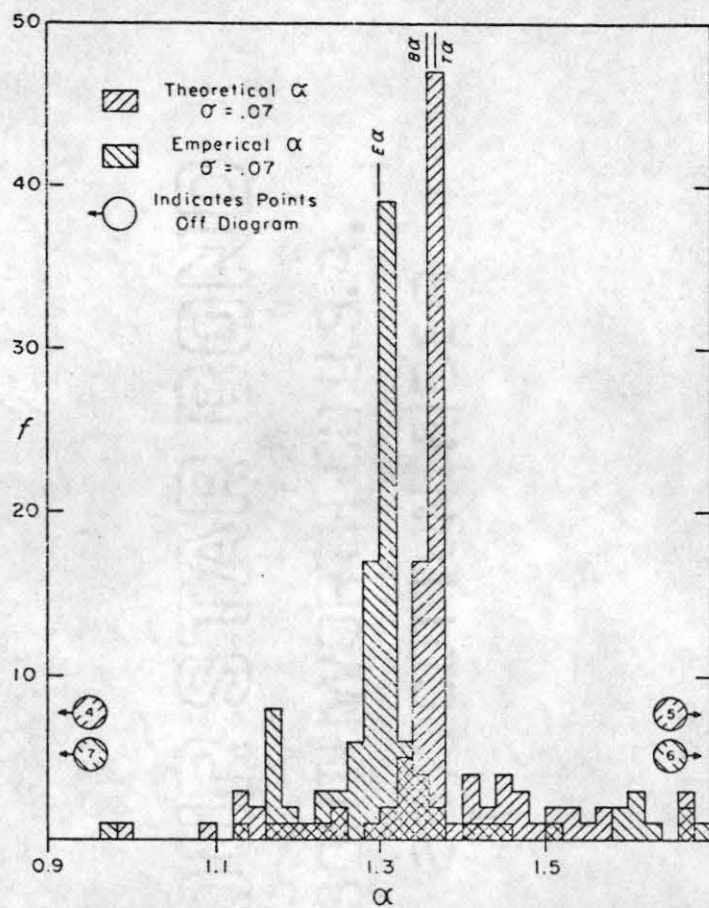
Table 5. Error Reduction Caused by Elimination of One Mix from Least Squares Solution at 15 KV.

α Factor	Error with All 10 Mixes	Error Using 9 Mixes	Mix Eliminated
$\alpha_{\text{Si}}^{\text{MgO}}$	$\pm .13$	$\pm .02$	J
$\alpha_{\text{Al}}^{\text{CaO}}$	$\pm .11$	$\pm .03$	G
$\alpha_{\text{Al}}^{\text{MgO}}$	$\pm .80$	$\pm .04$	J
$\alpha_{\text{Ca}}^{\text{Al}_2\text{O}_3}$	$\pm .06$	$\pm .03$	G
$\alpha_{\text{Ca}}^{\text{MgO}}$	$\pm .11$	$\pm .02$	J
$\alpha_{\text{Si}}^{\text{CaO}}$	$\pm .03$	$\pm .01$	G

graphically in Figures 10-21. For each alpha factor, the 120 theoretical or empirical values were divided into groups that consisted of all values in a 0.02 range. For example, all values of $\alpha_{\text{Si-CaO}}^{\text{Si}}$ (theoretical) such that $1.00 \leq \alpha_{\text{Si-CaO}}^{\text{Si}} < 1.02$ were included in one group. The abscissas of the histograms in Figures 10-21 represent the alpha factor (group) range and the ordinates represent frequency or number of alpha factor values per 0.02 range. For comparison, the theoretical ($T\alpha$) and empirical ($E\alpha$) alpha factors calculated by least squares from all ten mixes, and the theoretical binary alpha factors ($B\alpha$) are included on the diagrams.

An estimate of the standard deviations of each of the theoretical and empirical alpha factor distributions was made. These estimates are included in Figures 10-21. The estimates were made assuming that 68% of the total points should lie within $\pm\sigma$. Eighty-one points (0.68×120) were counted symmetrically about each peak (highest peak for that theoretical or empirical alpha factor). The included spread in the value of the alpha factor was divided by two giving an estimate of the standard deviation (σ). Table 6 compares the errors propagated by the least squares fit to ten mixes and the standard deviations calculated by the above method (method two).

No one composition seemed to control the distributions of alpha factors shown in Figures 10-21. Removing a mix with a low concentration of the "affecting" oxide reduced the standard deviation calculated by the least squares method. This is not true for the standard deviation calculated by method two. For example, removal of Mix J from



Distributions of theoretical and empirical alpha factor values versus frequency of those values. Distributions are derived from the 120 exact solutions of three linear equations.

Figure 10. Distributions for $\alpha_{\text{Si-MgO}}^{\text{Si}}$

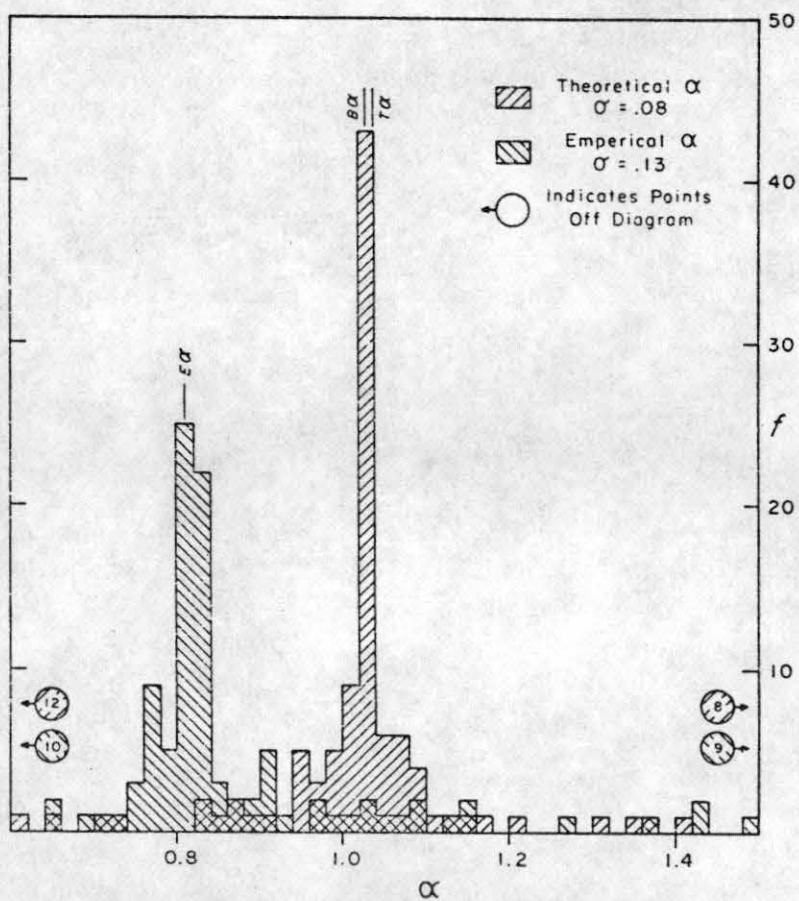


Figure 11. Distributions for $\alpha_{\text{Al-SiO}_2}^{\text{Al}}$

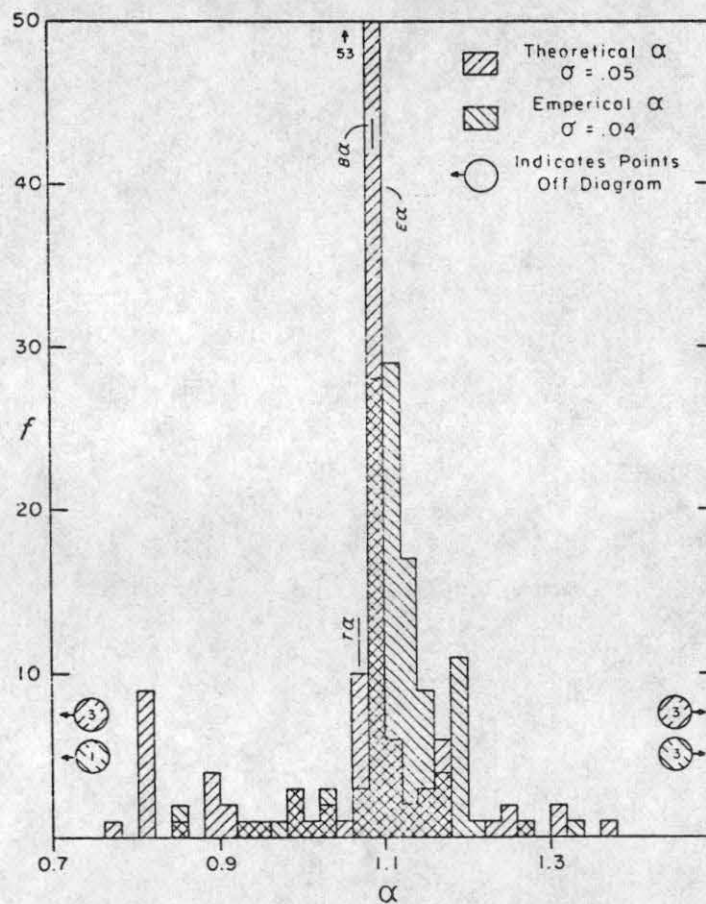


Figure 12. Theoretical and Empirical distributions for $\alpha_{\text{Ca-Ca-SiO}_2}$.

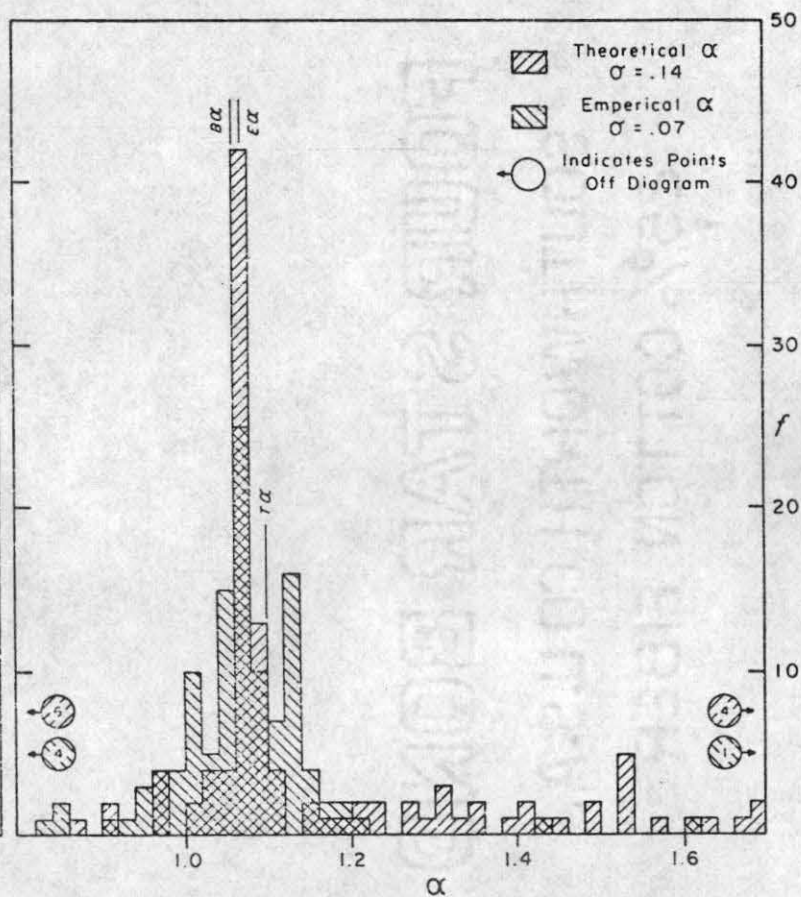


Figure 13. Theoretical and Empirical distributions for $\alpha_{\text{Ca-Ca-Al}_2\text{O}_3}$.

See Figure 10 and text for explanation.

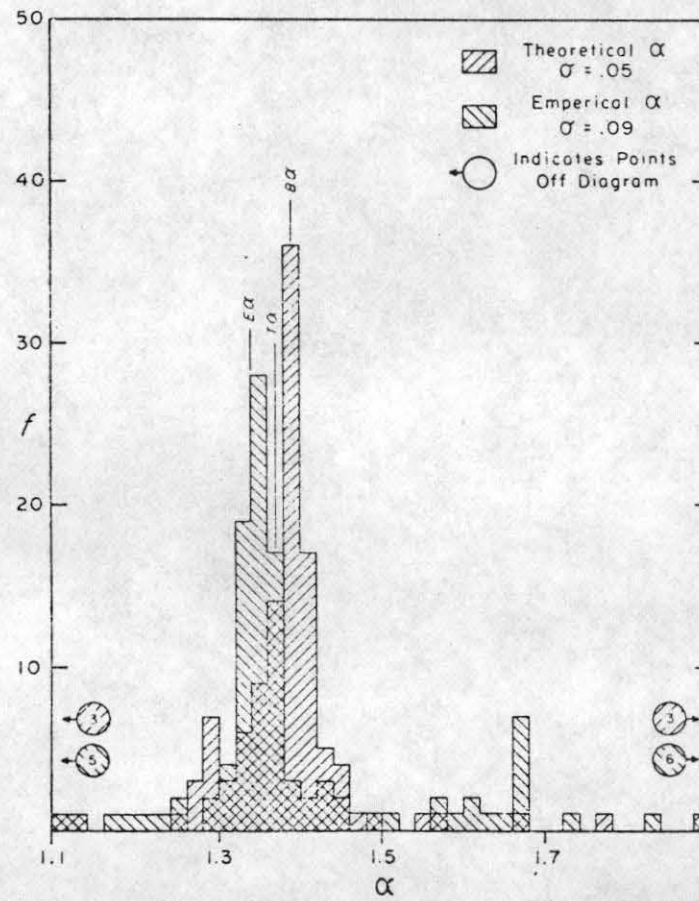


Figure 14. Theoretical and Empirical distributions for $\alpha_{Si} / Si-Al_2O_3$.

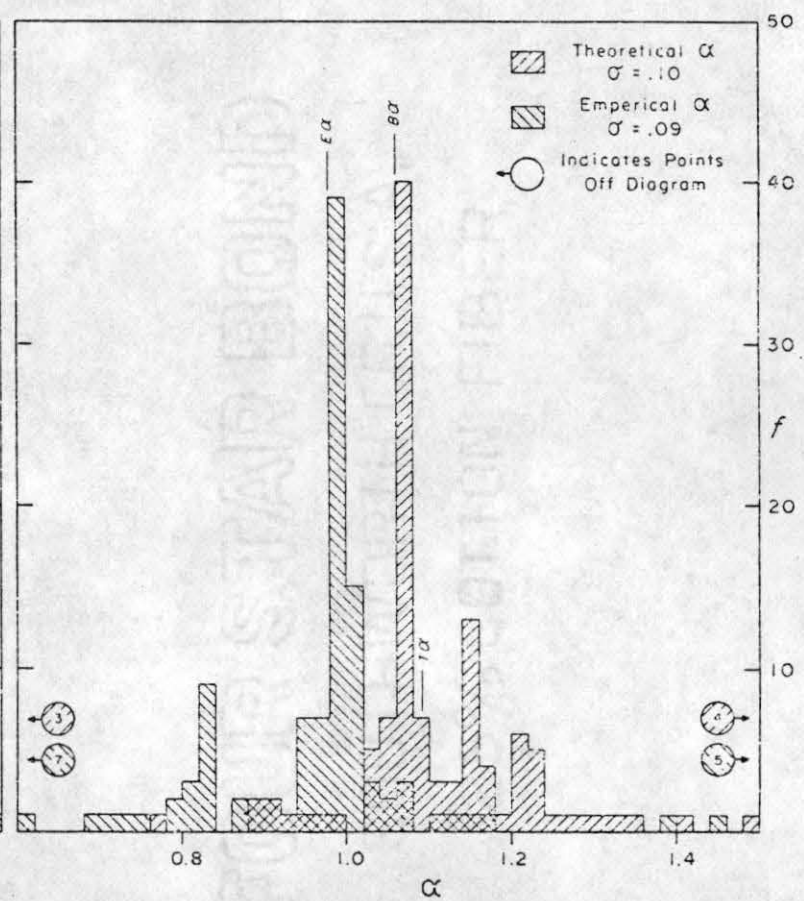


Figure 15. Theoretical and Empirical distributions for $\alpha_{Si} / Si-CaO$.

See Figure 10 and text for explanation.

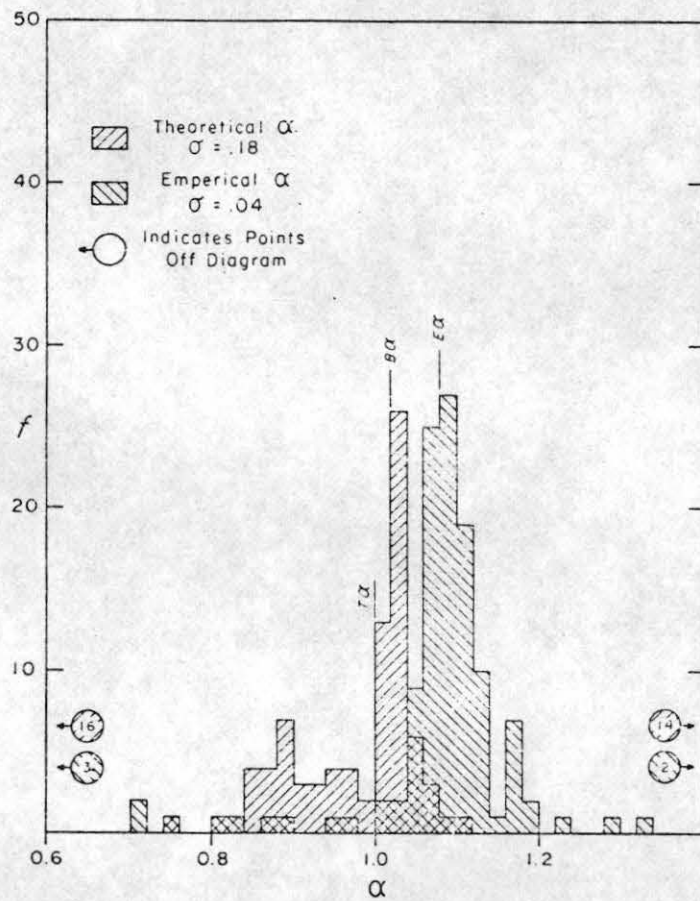


Figure 16. Theoretical and Empirical distributions for $\alpha_{\text{Mg-Mg-Al}_2\text{O}_3}$.

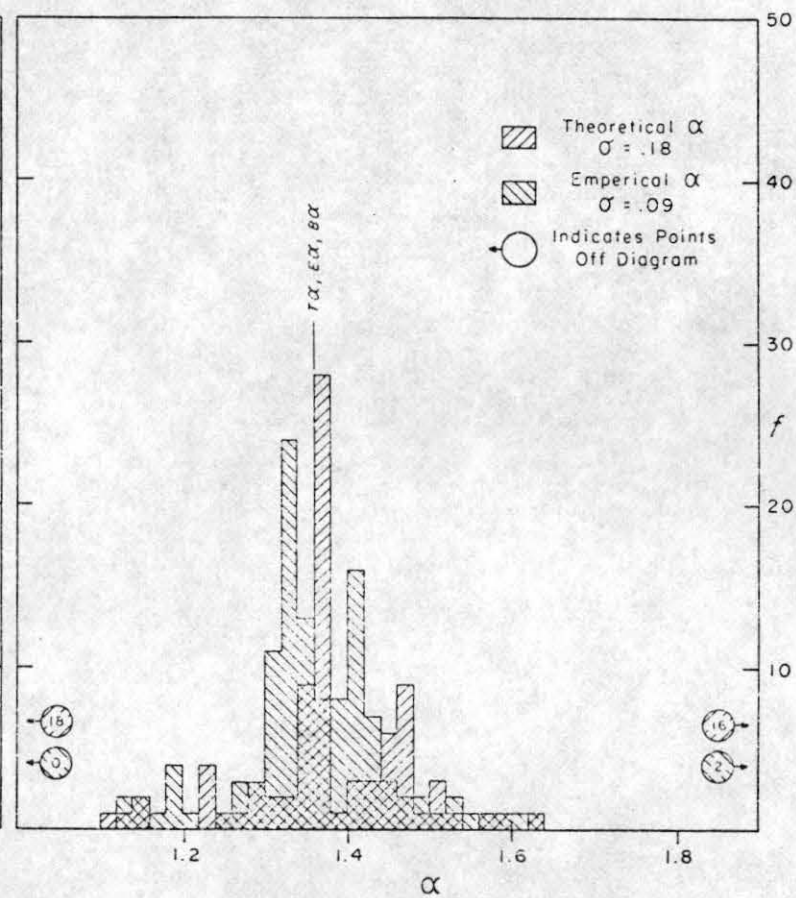


Figure 17. Theoretical and Empirical distributions for $\alpha_{\text{Mg-Mg-CaO}}$.

See Figure 10 and text for explanation.

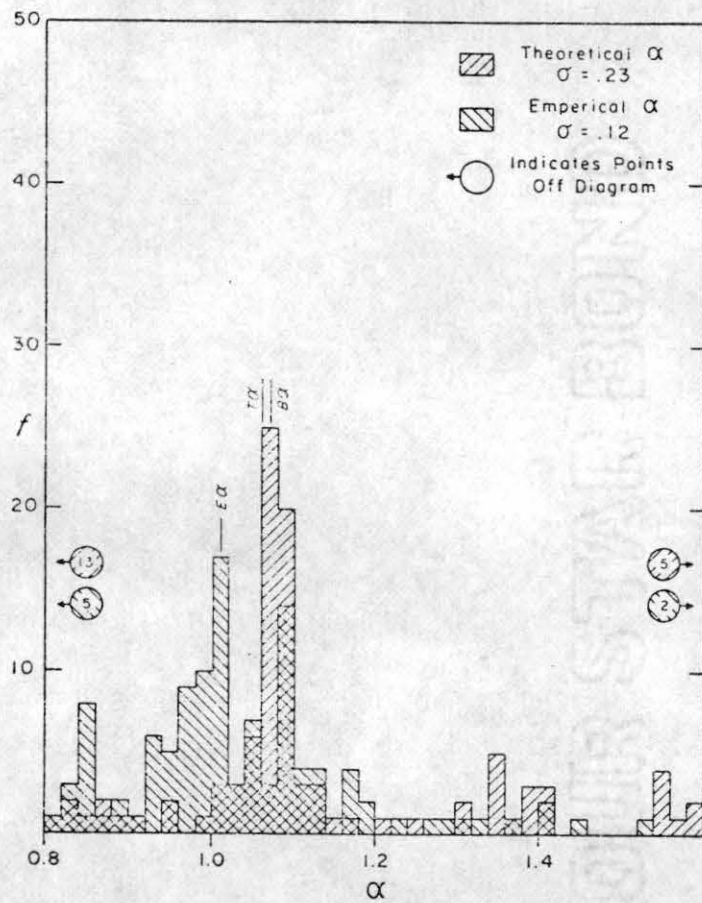


Figure 18. Theoretical and Empirical distributions for $\alpha_{\text{Ca}} / \text{Ca-MgO}$.

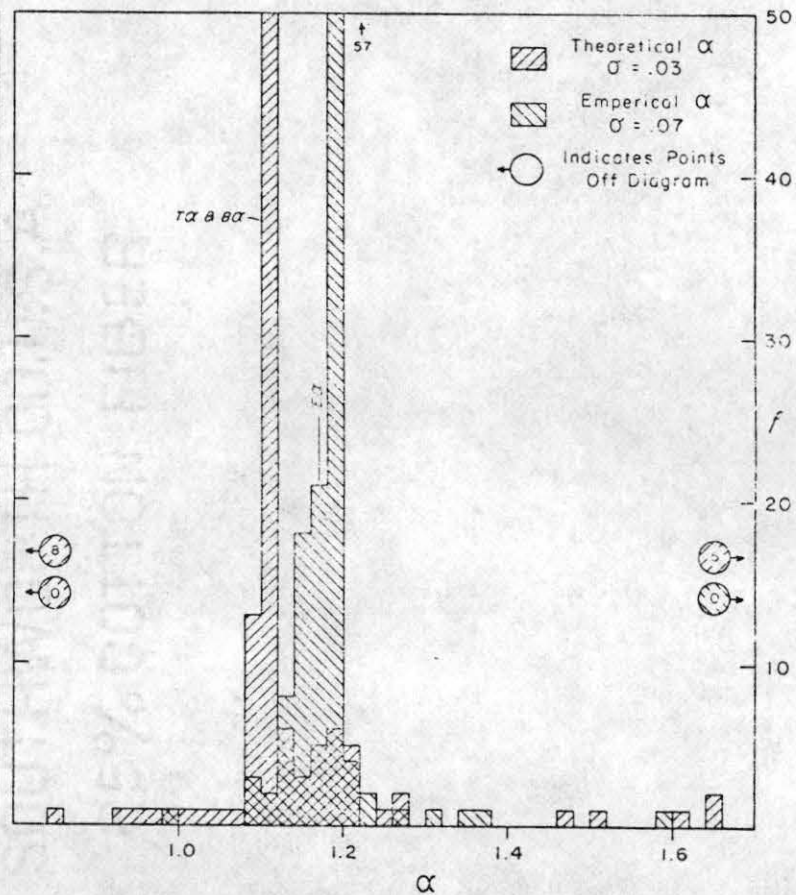


Figure 19. Theoretical and Empirical distributions for $\alpha_{\text{Mg}} / \text{Mg-SiO}_2$.

See Figure 10 and text for explanation.

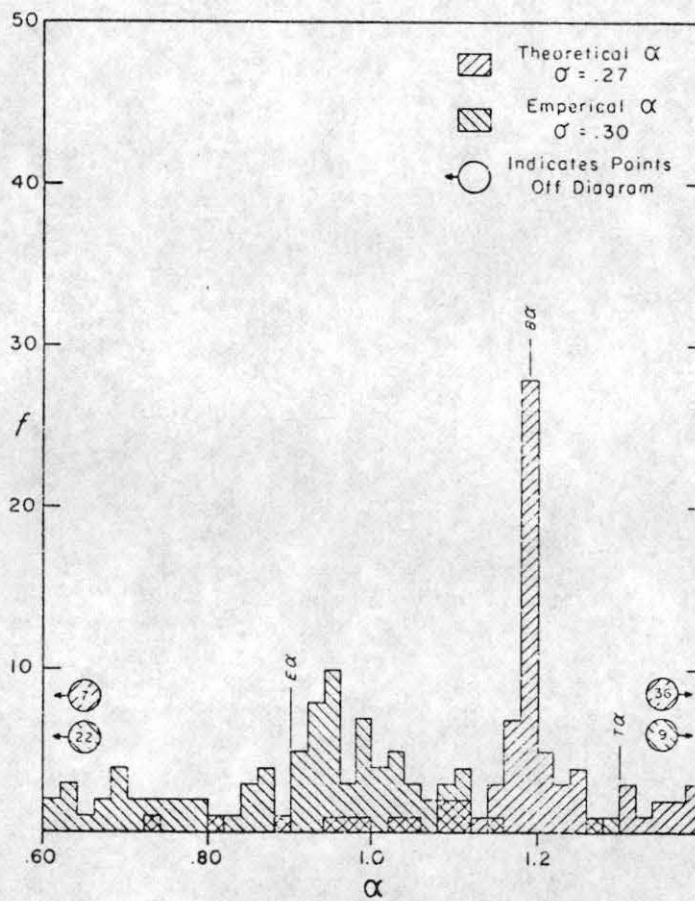


Figure 20. Theoretical and Empirical distributions for $\alpha_{\text{Al-CaO}}$.

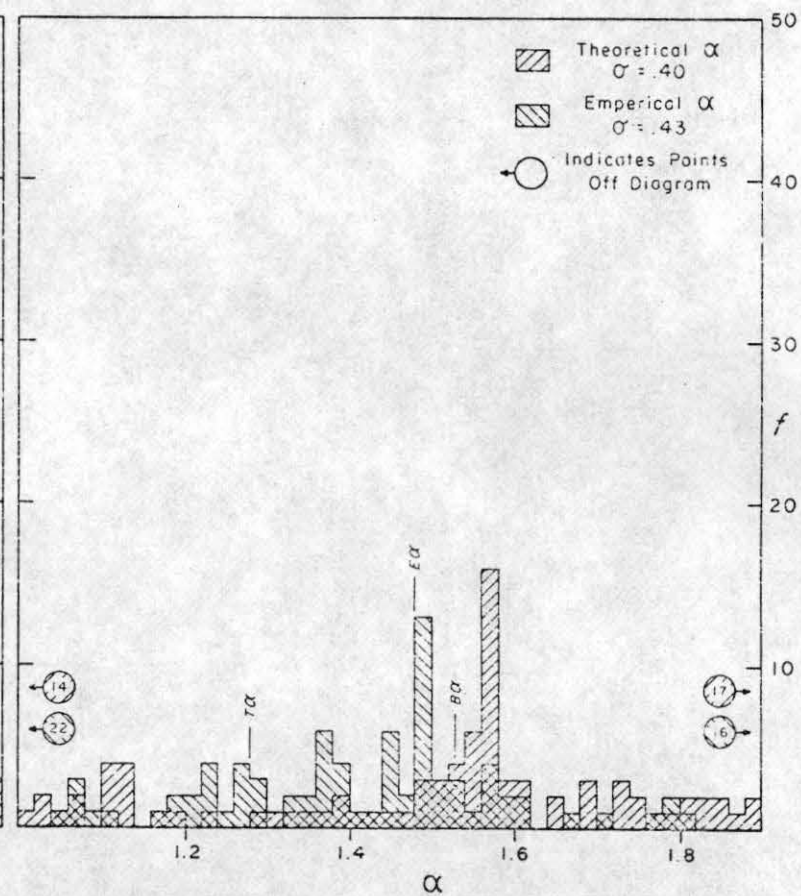


Figure 21. Theoretical and Empirical distributions for $\alpha_{\text{Al-MgO}}$.

See Figure 10 and text for explanation.

Table 6. Comparison of Standard Deviations by Least Squares Method and Method Two.

α Factor	$E\alpha^*$	Empirical Method 2	Theoretical Method 2
$\alpha_{\text{Si-Si-Al}_2\text{O}_3}^{\text{Si}}$	$\pm .03$	$\pm .09$	$\pm .05$
$\alpha_{\text{Si-Si-CaO}}^{\text{Si}}$	$\pm .01$	$\pm .09$	$\pm .10$
$\alpha_{\text{Si-Si-MgO}}^{\text{Si}}$	$\pm .02$	$\pm .07$	$\pm .07$
$\alpha_{\text{Al-Al-SiO}_2}^{\text{Al}}$	$\pm .003$	$\pm .13$	$\pm .08$
$\alpha_{\text{Al-Al-CaO}}^{\text{Al}}$	$\pm .03$	$\pm .30$	$\pm .27$
$\alpha_{\text{Al-Al-MgO}}^{\text{Al}}$	$\pm .04$	$\pm .43$	$\pm .40$
$\alpha_{\text{Ca-Ca-SiO}_2}^{\text{Ca}}$	$\pm .0007$	$\pm .04$	$\pm .05$
$\alpha_{\text{Ca-Ca-Al}_2\text{O}_3}^{\text{Ca}}$	$\pm .03$	$\pm .07$	$\pm .14$
$\alpha_{\text{Ca-Ca-MgO}}^{\text{Ca}}$	$\pm .02$	$\pm .12$	$\pm .23$
$\alpha_{\text{Mg-Mg-SiO}_2}^{\text{Mg}}$	$\pm .0004$	$\pm .03$	$\pm .07$
$\alpha_{\text{Mg-Mg-Al}_2\text{O}_3}^{\text{Mg}}$	$\pm .02$	$\pm .04$	$\pm .18$
$\alpha_{\text{Mg-Mg-CaO}}^{\text{Mg}}$	$\pm .01$	$\pm .09$	$\pm .18$

*See Table 5 and text.

the calculation of $\alpha_{\text{Si-MgO}}^{\text{Si}}$ reduced the uncertainty from 0.13 to 0.02 using the least squares method. Figure 22 shows that this reduction in uncertainty does not occur when Mix J is removed from the method two calculation. In fact, the standard deviation increases from 0.07 to 0.13 for both the theoretical and empirical alpha factors.

There does not seem to be a straightforward explanation for the differences between alpha factors predicted by various methods. The value of an alpha factor is apparently controlled by the complex inter-relationships of all constituents within the mixes and by the method used to calculate that factor. The question remains, "Which method produces the best alpha factors?" The definition of the best set of alpha factors is that set which best predicts the weight compositions of a broad range of mixes from X-ray intensities. Therefore, each set of alpha factors has been used to predict concentrations from the X-ray intensities.

This has already been done for Albee and Ray's alpha factors using Mix C as a standard (see Table 1) and the other mixes as unknowns. The X-ray intensities recorded during the run at 15KV accelerating potential used to calculate empirical alpha factors were used as the raw data (see Appendix 3, Table 9). The B-A α factors, the B α factors, the T α factors and the E α factors were each used to predict the compositions of Mixes A-J using Mix C as the standard. Table 7 compares the calculated compositions and the weighed-in compositions of the mixes. The differences: weighed-in composition minus calculated composition in percent of the weighed-in composition are listed. No one method consis-

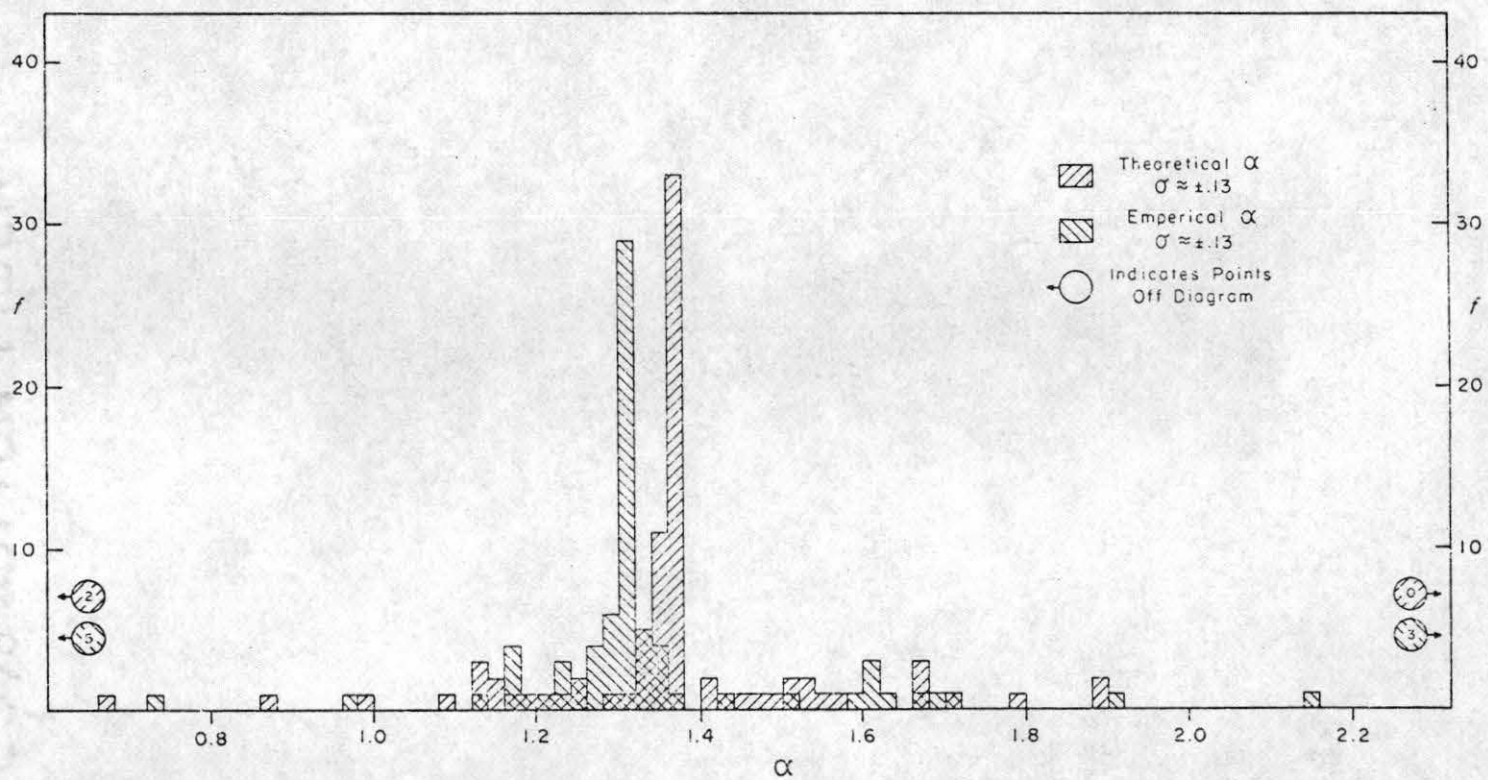


Figure 22. Theoretical and Empirical distributions for $\alpha_{\text{Si-Si-MgO}}$ with Mix J excluded from the set of exact solutions of three linear equations. See Figure 10 and the text for an explanation of the diagram construction.

tently gave the best answers for all oxides or even any one oxide. Mix E contains 80% SiO_2 . No one set of alpha factors seemed to be able to predict the composition of E using C as a standard. The empirical alpha factors came closest to predicting this extreme composition. Mix H contains almost 42% Al_2O_3 . Its composition was best predicted by the A-R and B-A alpha factors. To decide which method best predicted the nine compositions in the $\text{SiO}_2 - \text{Al}_2\text{O}_3 - \text{CaO} - \text{MgO}$ system, the differences listed in Table 7 were averaged over the nine mixes for each oxide. The sets with the lowest averages for each oxide are listed in Table 8. All averages within ten percent of the lowest average were considered to be the same. The $E\alpha$ factors best predicted SiO_2 values. Al_2O_3 was best predicted by the A- $R\alpha$ factors. If Mix H is eliminated from the average, the $E\alpha$ factors predict Al_2O_3 as well as the A- $R\alpha$ factors. CaO is predicted well by all five sets though the A- $R\alpha$ and $T\alpha$ factors give the best results. MgO is predicted well by all methods but the best results are given by the A- $R\alpha$ and the $E\alpha$ factors. The A- $R\alpha$ and $E\alpha$ factors seem to give the best overall results in this four component system.*

*Note: The compositions as calculated by the theoretical method could be compared to the compositions calculated by the various sets of alpha factors. See Appendix 3, Table 9 for the necessary information to do these calculations.

Table 7. Differences (in %) in Compositions as Predicted by Various Sets of Alpha Factors at 15 KV.

Method	SiO ₂	Al ₂ O ₃	CaO	MgO	Total
Mix A	49.72	16.07	23.15	11.05	100.00
A-R α	.14	.01	-.05	.01	.13
B-A α	.05	-.02	.01	.06	.11
B α	.06	-.09	-.06	-.04	-.12
T α	0.00	-.40	-.10	-.04	-.53
E α	.21	.11	-.13	-.03	.17
Mix B	48.99	16.05	20.97	13.99	100.00
A-R α	.11	.01	-.11	.04	.05
B-A α	.10	-.02	-.07	.08	.09
B α	.08	-.05	-.11	-.01	-.09
T α	.05	-.23	-.15	0.00	-.33
E α	.20	.02	-.14	.01	.09
Mix D	45.07	20.96	16.00	17.97	100.00
A-R α	-.01	0.00	-.09	-.04	-.14
B-A α	.22	-.03	-.04	.01	.16
B α	.11	.01	-.08	-.01	.03
T α	.17	.09	-.14	.01	.13
E α	.17	-.38	-.07	-.01	-.29
Mix E	79.97	8.99	5.04	6.00	100.00
A-R α	2.55	-.35	0.00	.09	2.29
B-A α	1.45	-.24	-.10	.01	1.12
B α	2.32	-.35	-.02	.14	2.10
T α	2.55	-.48	.02	.14	2.23
E α	1.18	-.03	-.06	.05	1.14
Mix F	52.06	30.93	6.94	10.07	100.00
A-R α	.22	.36	-.06	.01	.54
B-A α	.46	.47	-.10	-.02	.81
B α	.45	.36	-.06	.12	.87
T α	.74	.21	-.11	.15	.10
E α	.18	-.17	-.10	.04	.39

Table 7—continued

Method	SiO ₂	Al ₂ O ₃	CaO	MgO	Total
Mix G	61.12	3.31	2.89	32.69	100.00
A-R α	.43	.01	-.07	-.10	.26
B-A α	.56	.02	-.16	-.46	.05
B α	.56	.06	-.14	.24	.71
T α	.60	.21	-.11	.18	.87
E α	.18	0.00	-.12	.22	.27
Mix H	30.91	41.90	21.97	5.22	100.00
A-R α	-.39	.11	-.04	.04	-.28
B-A α	-.12	-.63	.12	.10	-.53
B α	-.28	-.80	-.02	.05	-1.05
T α	-.17	-2.12	-.38	.08	-2.59
E α	-.11	-2.34	-.19	.03	-2.69
Mix I	52.95	2.01	26.01	19.03	100.00
A-R α	.14	-.04	-.06	.04	.09
B-A α	-.14	-.05	.04	.11	-.04
B α	-.10	-.04	-.06	-.12	-.32
T α	-.36	-.06	.07	-.15	-.50
E α	.09	0.00	.01	.03	.13
Mix J	42.98	19.02	36.99	1.01	100.00
A-R α	.03	-.08	.21	.02	.18
B-A α	-.24	-.25	.48	.03	.01
B α	-.17	-.42	.18	.01	-.40
T α	-.41	-1.55	-.03	0.00	-1.99
E α	.30	.27	-.12	.01	-.46

Table 8. Sets of Alpha Factors Which Show the Average Lowest Difference (from Table 7) for Individual Oxides.

SiO ₂	Al ₂ O ₃	CaO	MgO
E α (0.29)	A-R α (0.11)	A-R α (0.08)	A-R α (0.04)
	E α (0.12)*	B α (0.07)	E α (0.05)

*Average calculated without Mix H.

CONCLUSION

The purpose of this project was twofold - to produce a set of reliable microprobe standards of use to geologists and to calculate a set of empirical correction (alpha) factors for microprobe data reduction. Ten homogeneous glasses in the system: $\text{SiO}_2 - \text{Al}_2\text{O}_3 - \text{CaO} - \text{MgO}$ were synthesized. The compositions of these standards were taken directly from the weighed-in concentrations of the end member oxides and verified by microprobe analysis. The empirical alpha factors calculated for this project have been shown to be as accurate as published alpha factors in predicting compositions within the four component system.

The values and precision of these twelve alpha factors might be improved by repeated calculations using different microprobe runs at set conditions for a constant set of mixes. The values of the twelve alpha factors could be tested by using them to reduce microprobe data for more complex silicate systems. The method of alpha factor generation could be applied to other, more complex silicate systems. Perhaps, the next logical oxides to add to the system studied are Na_2O , K_2O , FeO and TiO_2 since these oxides comprise a significant proportion of many rocks and minerals.

Appendix 1. Sample Preparation Notes

- Mix A
1. Oxide mixture was stirred slightly and fused for approximately 3 hours at 1650°C . The mix appeared glassy after the run. ("glassy" = clear, non-crystalline at approx. 0.1mm scale)
 2. Glass was broken in crucible into several mm size pieces and run for $2\frac{1}{2}$ hours at approximately 1650°C . It appeared glassy after the run.
 3. Glass was broken in crucible and then in a hardened steel cylinder. It was run for $2\frac{1}{2}$ hours at 1650°C . It appeared glassy after the run.
 4. The glass was stored in a dessicator on 27 July, 1976.
- Mix B
1. The oxide mixture was stirred, then fused for $2\frac{1}{2}$ hours at approximately 1650°C . The mix appeared glassy after the run.
 2. The glass was broken in the crucible and in the steel cylinder. It was run for $2\frac{1}{2}$ hours at the same temperature. It appeared glassy after the run.
 3. The glass was broken and re-run as in step 2. It appeared glassy after the run.
 4. The glass was stored in the dessicator on 27 July, 1976.

Appendix 1. continued

- Mix C
1. The oxide mixture was stirred and run for 2.33 hours at approximately 1600°C . It appeared glassy after the run.
 2. The mixture was broken into mm size pieces in the crucible and run for 2.33 hours at approximately 1650°C . It appeared glassy after the run.
 3. The mix was broken and re-run as in step 2. It appeared glassy after the run.
 4. The mix was stored in the dessicator on 15 June, 1976.

- Mix D
1. The mixture was stirred and run at approximately 1650°C for 3 hours. It appeared glassy after the run.
 2. The glass was broken in the crucible and run at the same temperature for $2\frac{1}{2}$ hours. It appeared glassy after the run.
 3. The glass was broken and re-run as in step 2. It appeared glassy after the run.
 4. The glass was stored in the dessicator on 29 July, 1976.

- Mix E
1. The oxide mixture was stirred and run at approximately 1600°C for 2 hours. Apparently, some undissolved material remained after the run.
 2. The mix was broken in the crucible and re-run as in step 1 with the same results.

Appendix 1. continued

3. The mix was run twice at approximately 1650°C for 2 hours each time. Some undissolved material and/or crystallites remained after each run.
4. The mix was ground under alcohol in an agate mortar into 0.1 mm size pieces. It was run at 1650°C for 2 hours and appeared glassy after the run.
5. The mix was ground and run twice more as in step 4. It appeared glassy after each run.
6. The mix was proven inhomogeneous by the microprobe check.
7. The mix was re-ground under alcohol in an agate mortar, then run at approximately 1700°C for one hour. It appeared glassy after the run.
8. The glass was stored in a dessicator on 1 August, 1976, after proving to be homogeneous by microprobe check.

Mix F

1. The oxide mix was stirred and run for $2\frac{1}{2}$ hours at approximately 1650°C . Some undissolved material was observed after the run.
2. The mix was broken in the crucible and run for 2.75 hours at approximately 1670°C . It appeared glassy after the run.
3. The glass was broken and run as in step 2 for $2\frac{1}{2}$ hours. It appeared glassy after the run.

Appendix 1. continued

4. The glass was broken and run as in step 3 for 2 hours. It appeared glassy after the run.
5. The glass was stored in the dessicator on 15 June, 1976.

Mix G

1. The oxide mixture was stirred and run for 3 hours at approximately 1650°C. It appeared milky after the run.
2. The mix was broken in the crucible and run for 2.33 hours at approximately 1670°C. It still appeared milky after the run.
3. The mix was crushed in the steel cylinder and ground slightly (to "gritty" texture) under alcohol in an agate mortar. It was run for 2½ hours at approximately 1670°C. It appeared milky after the run.
4. Step 3 was repeated but the temperature was raised to 1700°C. The mix appeared milky after the run.
5. Approximately 1/3 of the mix was run for 1½ hours at about 1730°C but had the same homogeneous, cloudy appearance after the run.
6. The mix was shown to be homogeneous by microprobe check inspite of its cloudy appearance and was stored in the dessicator on 29 July, 1976.

Appendix 1. continued

- Mix H
1. The oxide mixture was stirred and run for 3 hours at approximately 1650°C. Some undissolved material was observed after the run.
 2. The mix was broken in the crucible and run for 2½ hours at approximately 1650°C. It appeared glassy after the run.
 3. The glass was broken and run as in step 2 two more times. It appeared glassy after each run.
 4. The mix was stored in the dessicator on 19 July, 1976.

- Mix I
1. The oxide mixture was stirred and run for 2½ hours at approximately 1650°C. It appeared glassy after the run.
 2. The mix was broken in the crucible and run for 2½ hours at approximately 1650°C. It appeared glassy after the run.
 3. Step 2 was repeated. The mix appeared glassy after the run.
 4. The mix was stored in the dessicator on 8 June, 1976.

- Mix J
1. The oxide mixture was stirred and run for 2½ hours at approximately 1650°C. It appeared glassy after the run.
 2. The mix was broken in the crucible and run for 2½ hours at approximately 1650°C. It appeared glassy after the run.

Appendix 1. continued

3. Step 2 was repeated. The mix appeared glassy after the run.
4. The glass was stored in the dessicator on 10 June, 1976.

-
- Note:
1. Mixes broken in the crucible were broken into pieces several mm across. Mixes crushed in the steel cylinder were broken into somewhat smaller pieces - about 1-2mm.
 2. Unless otherwise stated, all mixes were shown to be homogeneous by the first microprobe check.

Appendix 2. Theoretical (ZAF) Correction Method Using a Pure Element Standard, with n elements in the mix and m is the element analyzed. (Yakowitz, 1975)

I. Atomic Number Correction (Z)

$$A. R1 = (8.73 \times 10^{-3} \times (V/E_m)^3) - (0.1669 \times (V/E_m)^2) + (0.9662 \times (V/E_m)) + 0.4523$$

$$R2 = (2.70 \times 10^{-3} \times (V/E_m)^3) - (5.182 \times 10^{-2} \times (V/E_m)^2) + (0.302 \times (V/E_m)) - 0.1836$$

$$R3 = ((0.887 \times (V/E_m)^3) - (3.44 \times (V/E_m)^2) + (9.33 \times (V/E_m)) - 6.43) / ((V/E_m)^3)$$

$$R = \sum_{i=1}^n \{C_i \times (R1 - (R2 \times \log((R3 \times N_i) + 25)))\}$$

where

V is the accelerating potential in KV.

E_m is the critical excitation potential of "m" in KV.

N_i equals the atomic number of element i .

C_i equals the weight fraction of element i in the mix.

R equals the backscatter correction for the unknown.

$$R' = R1 - (R2 - \log((R3 \times N_m) + 25))$$

where

R' is the backscatter for the pure element standard.

$$B. S = \sum_{i=1}^n \{C_i \times (N_i / (W_i \times (V + E_m))) \times \log(583 \times (V + E_m) / J_i)\}$$

$$J_i = (9.76 \times N_i) + (58.8 \times N_i^{-0.19})$$

$$S' = (N_m / (W_m \times (V + E_m))) \times \log(583 \times (V + E_m) / J_m)$$

where

W_i = the atomic weight of element i .

S = the atomic stopping power for the unknown.

S' = the stopping power for the pure element standard.

Appendix 2. continued

$$C. Z = (S \times R') / (S' \times R)$$

II. The Absorption Correction (A)

$$A. \chi = \sum_{i=1}^n \{M_{m,i} \times C_i \times 1,2605\}$$

1.2605 = cosec(52.5°) where 52.5° is the take-off angle.

$$\chi' = M_{m,m} \times 1.2605$$

$$P = 1 \div (1 + (3 \times 10^{-6} \times (\nu^{1.65} - E_m^{1.65}) \times \chi) +$$

$$(4.5 \times 10^{-13} \times (\nu^{1.65} - E_m^{1.65})^2 \times \chi^2))$$

P' = P when χ' is substituted for χ .

where

$M_{x,y}$ is the mass absorption coefficient; y is the absorber.

P is the correction for the unknown.

P' is the correction for the standard.

$$B. A = P'/P \text{ --- the absorption correction.}$$

Appendix 2. continued

III. The Fluorescence Correction (F)

- A. For energy of the "excitor" greater than E_m . "i" stands for the excitor.

$$B = (0.88 \times \omega_i \times W_m) / W_i$$

$$D = ((V/E_i) - 1) / ((V/E_m) - 1)^{1.67}$$

$$S1 = \sum_{j=1}^n \{C_j \times M_{i,j}\}$$

$$S2 = \sum_{j=1}^n \{C_j \times M_{m,j}\}$$

$$G1 = \log((1 + (1.2605 \times S2/S1)) / (1.2605 \times S2/S1))$$

$$G2 = \log\left\{ \frac{(1 + (3.3 \times 10^5 / (V^{1.65} - (E_m^{1.65} \times S1))))}{(3.3 \times 10^5 / (V^{1.65} - (E_m^{1.65} \times S1)))} \right\}$$

$$G_{m,i} = (C_i \times B \times D \times M_{i,m}) / (S1 \times (G1 + G2))$$

B. $F = 1 / \{1 + (\sum_{i=1}^n G_{m,i})\}$

- C. ω is the fluorescent yield and F is the fluorescence correction.

- D. There is no fluorescence correction for the pure element standard.

IV. The Completed Theoretical Correction

$$C_m / C' = (I_m / I') \times Z \times A \times F$$

where

C_m = weight fraction of element m in the unknown.

C' = the weight fraction of element m in the standard ($\cong 1$).

I_m = characteristic X-ray intensity produced by element m in the unknown.

I' = that X-ray intensity produced by element m in the pure element standard.

Appendix 2. continued

V. The Constants used for the Theoretical Correction

W = atomic weight

ω = fluorescent yield

$M_{x,y}$ = the mass absorption coefficient; y is the absorber.

E_i = the critical excitation potential in KV of element i .

A. Oxygen

$W = 15.9994$, $\omega = 0.0022$, $E_O = 0.532$

$M(O,O) = 1340$

$M(O,Mg) = 5680$

$M(O,Al) = 6830$

$M(O,Si) = 8770$

$M(O,Ca) = 29900$

B. Magnesium

$W = 24.312$, $\omega = 0.03$, $E_{Mg} = 1.303$

$M(Mg,O) = 2620$

$M(Mg,Mg) = 555$

$M(Mg,Al) = 661$

$M(Mg,Si) = 888$

$M(Mg,Ca) = 2980$

C. Aluminum

$W = 26.9815$, $\omega = 0.04$, $E_{Al} = 1.56$

$M(Al,O) = 1620$

$M(Al,Mg) = 4040$

$M(Al,Al) = 410$

$M(Al,Si) = 555$

$M(Al,Ca) = 1850$

D. Silicon

$W = 28.086$, $\omega = 0.055$, $E_{Si} = 1.84$

$M(Si,O) = 1060$

$M(Si,Mg) = 2780$

$M(Si,Al) = 3340$

$M(Si,Si) = 365$

$M(Si,Ca) = 1220$

Appendix 2. continued

E. Calcium

$$W = 40.08, \omega = 0.19, E_{Ca} = 4.038$$

$$M(\text{Ca}, \text{O}) = 122$$

$$M(\text{Ca}, \text{Mg}) = 390$$

$$M(\text{Ca}, \text{Al}) = 475$$

$$M(\text{Ca}, \text{Si}) = 590$$

$$M(\text{Ca}, \text{Ca}) = 165$$

Appendix 3. Data used in the Linear Least Squares Program and the errors propagated by that method.

- I. Tables 9, 10 and 11 list the data just as it was input in the least squares program. The data was used to solve a set of linear equations of the form:

$$\sum_{i \neq n} C_u^i \alpha_{n-i}^n = B$$

where

$$B = (k_u^n/k_n^n) - C_u^n.$$

k_u^n/k_n^n is the observed intensity ratio in Tables 9 and 10.

k_u^n/k_n^n is the theoretically calculated intensity ratio in

Table 11. By substituting the appropriate B's (at a particular accelerating potential; empirical or theoretical) into Table 9, each line represents an equation - one set of $\{C_i, \text{difference}\}$ input in the linear least squares program to produce empirical or theoretical alpha factors at that accelerating potential.

Given B for element n in Mix u, the intensity ratio - k_u^n/k_n^n - can be simply obtained:

$$B + C_u^n = k_u^n/k_n^n.$$

The k ratios obtained from Table 9 may be used to theoretically calculate mix compositions at 15KV and compare with the compositions calculated by the Bence-Albee method, pages 52-56.

Ratios rather than individual X-ray intensities (counts) were included in this appendix because the ratios might be reproduced.

- II. Tables 12, 13, 14, 15 and 16 list the errors (by equation) propagated by the least squares method. Errors for theoretical alpha factors are negligible so only those at 15KV are listed as an example.

Table 9. Empirical Alpha Factor Data (15KV) Used in Solution of Ten Linear Equations.

Element Analyzed	Mix	C _{SiO₂ mix}	C _{Al₂O₃ mix}	C _{CaO mix}	C _{MgO mix}	B	S.D. of B
Si	A	—	.160740	.231517	.110547	.5878	±.0083
Si	B	—	.160520	.209730	.139883	.6043	±.0105
Si	C	—	.139750	.169639	.169336	.5710	±.0087
Si	D	—	.209604	.159953	.179720	.6738	±.0104
Si	E	—	.089880	.050432	.059976	.2616	±.0093
Si	F	—	.309256	.069410	.100725	.6155	±.0167
Si	G	—	.033063	.028875	.326880	.4979	±.0123
Si	H	—	.418957	.219741	.052230	.8416	±.0133
Si	I	—	.020056	.260093	.190327	.5284	±.0078
Si	J	—	.190180	.369943	.010120	.6343	±.0108
Al	A	.497197	—	.231517	.110547	.7862	±.0197
Al	B	.489858	—	.209739	.139883	.7986	±.0237
Al	C	.521575	—	.169639	.169336	.8304	±.0216
Al	D	.450723	—	.159953	.179720	.7627	±.0203
Al	E	.799712	—	.050432	.059976	.7838	±.0111
Al	F	.520609	—	.069410	.100725	.6241	±.0226
Al	G	1.611182	—	.028875	.326880	1.0083	±.0263
Al	H	.309072	—	.219741	.052230	.4806	±.0186
Al	I	.529524	—	.260093	.190327	.9500	±.0424
Al	J	.429757	—	.369943	.010120	.7131	±.0279
Ca	A	.497197	.160740	—	.110547	.8357	±.0094
Ca	B	.489858	.160520	—	.139883	.8559	±.0087
Ca	C	.521275	.139750	—	.169336	.9051	±.0102
Ca	D	.450723	.209604	—	.179720	.9076	±.0107
Ca	E	.799712	.089880	—	.059976	1.0358	±.0164
Ca	F	.520609	.309256	—	.100725	1.0015	±.0199
Ca	G	.611182	.033063	—	.326880	1.0322	±.0196
Ca	H	.309072	.418957	—	.052230	.8435	±.0119
Ca	I	.529524	.020056	—	.190327	.8074	±.0083
Ca	J	.429757	.190180	—	.010120	.6939	±.0095
Mg	A	.497197	.160740	.231517	—	1.0642	±.0100
Mg	B	.489858	.160520	.209739	—	1.0296	±.0098
Mg	C	.521275	.139750	.169639	—	.9882	±.0079
Mg	D	.450723	.209604	.159953	—	.9683	±.0088
Mg	E	.799712	.089880	.050432	—	1.1069	±.0114
Mg	F	.520609	.309256	.069410	—	1.0368	±.0116
Mg	G	.611182	.033063	.028875	—	.7938	±.0058
Mg	H	.309072	.418957	.219741	—	1.1184	±.0054
Mg	I	.529524	.020056	.260093	—	.9921	±.0074
Mg	J	.429757	.190180	.369943	—	1.2202	±.0152

Note. The standard deviation of each oxide in Glasses A, B, C, D, F & H = ± .000005 and in Glasses E, G, I, & J = ± .000002.

Table 10. Empirical "B" Used in Solution of Ten Linear Equations by Least Squares Method at 10, 20 and 30 KV.

Element Analyzed	Mix	B 10KV	Standard Deviation	B 20KV	Standard Deviation	B 30KV	Standard Deviation
Si	A	.5379	.0136	.6109	.0151	.8556	.0107
Si	B	.5491	.0132	.6424	.0252	.8925	.0317
Si	C	.5240	.0159	.6193	.0120	.8511	.0163
Si	D	.6083	.0162	.7487	.0208	1.0200	.0168
Si	E	.2367	.0138	.2868	.0089	.4021	.0087
Si	F	.5430	.0183	.7180	.0145	.9738	.0159
Si	G	.4385	.0130	.5572	.0116	.7789	.0111
Si	H	.7619	.0167	.9459	.0179	1.3021	.0075
Si	I	.4987	.0122	.5634	.0097	.7454	.0107
Si	J	.6043	.0154	.6804	.0158	.8813	.0140
Al	A	.8912	.0241	.9976	.0151	1.1601	.0131
Al	B	.9116	.0258	1.0314	.0142	1.2121	.0165
Al	C	.9305	.0197	1.0566	.0175	1.2615	.0167
Al	D	.8711	.0301	1.0045	.0155	1.2063	.0182
Al	E	.9020	.0285	.9523	.0182	1.0402	.0185
Al	F	.7306	.0228	.8090	.0158	.9392	.0197
Al	G	1.0838	.0530	1.2988	.0377	1.5645	.0465
Al	H	.6175	.0190	.6860	.0111	.8110	.0112
Al	I	1.0451	.0058	1.2061	.0301	1.3999	.0505
Al	J	.8431	.0337	.9050	.0284	1.0369	.0151
Ca	A	.8014	.0198	.8781	.0091	.9231	.0081
Ca	B	.8217	.0178	.8949	.0099	.9421	.0076
Ca	C	.8770	.0142	.9431	.0103	.9961	.0104
Ca	D	.8734	.0194	.9476	.0100	.9910	.0448
Ca	E	1.0077	.0289	1.0717	.0125	1.1294	.0138
Ca	F	.9645	.0201	1.0401	.0143	1.0972	.0138
Ca	G	1.0104	.0450	1.0789	.0171	1.1179	.0137
Ca	H	.8113	.0131	.8791	.0083	.9287	.0084
Ca	I	.7913	.0187	.8431	.0070	.8897	.0066
Ca	J	.6679	.0154	.7309	.0072	.7729	.0067
Mg	A	1.0268	.0118	1.1338	.0113	1.2245	.0113
Mg	B	.9878	.0091	1.0846	.0097	1.1725	.0074
Mg	C	.9495	.0119	1.0386	.0078	1.1133	.0059
Mg	D	.9330	.0076	1.0157	.0072	1.0841	.0089
Mg	E	1.0723	.0129	1.1587	.0124	1.2123	.0108
Mg	F	1.0089	.0111	1.0748	.0083	1.1198	.0089
Mg	G	.7703	.0063	.7922	.0058	.8311	.0062
Mg	H	1.0763	.0123	1.1706	.0087	1.2432	.0033
Mg	I	.9416	.0067	1.0579	.0090	1.1338	.0074
Mg	J	1.1175	.0254	1.3075	.0174	1.3806	.0194

Table 11. Theoretical Alpha Factor Data at 10, 15, 20, and 30 KV Used in Linear Least Squares Solutions of Ten Equations.

Element Analyzed	Mix	B 10KV	B 15KV	B 20KV	B 30KV
Si	A	.5600	.62047	.6895	1.1176
Si	B	.5837	.64943	.7233	1.1252
Si	C	.5403	.60305	.6726	1.0005
Si	D	.6286	.70593	.7907	1.1413
Si	E	.2311	.26038	.2918	.3943
Si	F	.5625	.64052	.7235	.9480
Si	G	.4587	.52062	.5852	.7149
Si	H	.7889	.88723	.9964	1.5209
Si	I	.5320	.58198	.6409	1.1091
Si	J	.6161	.67272	.7416	1.4537
Al	A	.9007	.95732	1.0368	.7536
Al	B	.9207	.98427	1.0688	.8167
Al	C	.9338	.99814	1.0795	.8823
Al	D	.8673	.93256	1.0137	.8333
Al	E	.9427	.97392	1.0110	.9456
Al	F	.7353	.77370	.8189	.7450
Al	G	1.0827	1.04330	1.2661	1.3554
Al	H	.6202	.65894	.7179	.4447
Al	I	1.0884	1.16920	1.2792	.9503
Al	J	.8499	.89547	.9767	.5524
Ca	A	.8186	.83136	.8516	.9075
Ca	B	.8513	.86424	.8850	.9425
Ca	C	.8832	.89663	.9182	.9778
Ca	D	.8933	.90652	.9279	.9871
Ca	E	1.0086	1.02570	1.0523	1.1250
Ca	F	.9890	1.00430	1.0285	1.0958
Ca	G	1.0359	1.05130	1.0761	1.1451
Ca	H	.8262	.83832	.8579	.9124
Ca	I	.7422	.75356	.7718	.8222
Ca	J	.6709	.68167	.6987	.7455
Mg	A	.9533	1.02450	1.2243	.9424
Mg	B	.8626	.92488	1.0948	.8572
Mg	C	.8989	.95929	1.1137	.9063
Mg	D	.8700	.92576	1.0677	.8759
Mg	E	.9910	1.03860	1.1276	1.0538
Mg	F	.9377	.98084	1.0693	.9780
Mg	G	.7101	.74373	.8026	.7610
Mg	H	.9992	1.06460	1.2489	.9849
Mg	I	.8993	.97818	1.2121	.8750
Mg	J	1.0709	1.16760	1.4874	1.0217

Table 12. Standard Deviations (σ) of the Twelve Empirical Alpha Factors Propagated by the Least Squares Solution of Ten Equations. The error propagated for each equation is listed. (at 15 KV)

σ of the Following Alpha Factors:

	$\alpha_{\text{Si-Al}_2\text{O}_3}^{\text{Si}}$	$\alpha_{\text{Si-CaO}}^{\text{Si}}$	$\alpha_{\text{Si-MgO}}^{\text{Si}}$	$\alpha_{\text{Al-SiO}_2}^{\text{Al}}$	$\alpha_{\text{Al-CaO}}^{\text{Al}}$	$\alpha_{\text{Al-MgO}}^{\text{Al}}$	$\alpha_{\text{Ca-SiO}_2}^{\text{Ca}}$	$\alpha_{\text{Ca-Al}_2\text{O}_3}^{\text{Ca}}$	$\alpha_{\text{Ca-MgO}}^{\text{Ca}}$	$\alpha_{\text{Mg-SiO}_2}^{\text{Mg}}$	$\alpha_{\text{Mg-Al}_2\text{O}_3}^{\text{Mg}}$	$\alpha_{\text{Mg-CaO}}^{\text{Mg}}$
A	.002666	.001285	.005638	.001570	.007241	.031758	.000357	.003420	.007232	.000405	.003871	.001866
B	.004279	.002506	.005634	.002341	.012768	.028706	.000315	.002938	.003868	.000400	.003727	.002183
C	.003876	.002630	.002640	.001717	.016213	.016271	.000383	.005327	.003628	.000230	.003196	.002169
D	.002462	.004227	.003349	.002028	.016107	.012758	.000564	.002602	.003545	.000381	.001763	.003027
E	.010706	.034006	.024044	.000193	.048444	.034253	.000421	.033294	.074771	.000203	.016087	.051098
F	.002916	.057888	.027489	.001884	.106017	.050343	.001461	.004141	.039033	.000496	.001407	.027931
G	.138397	.181455	.001416	.001852	.829603	.006473	.001028	.351424	.003595	.000090	.030775	.040350
H	.001008	.003663	.064845	.003622	.007165	.126820	.001482	.000807	.051912	.000305	.000166	.000604
I	.151258	.000899	.001680	.006412	.026575	.049628	.000246	.171279	.001902	.000195	.136160	.000809
J	.003225	.000852	1.139048	.004215	.005689	7.600763	.000489	.002495	.881396	.001251	.006388	.001688

Table 13. Standard Deviations (σ) of the Twelve Empirical Alpha Factors Propagated by the Least Squares Solution of Ten Equations. (10 KV)

σ of the Following Alpha Factors:

	$\alpha_{\text{Si-Al}_2\text{O}_3}^{\text{Si}}$	$\alpha_{\text{Si-CaO}}^{\text{Si}}$	$\alpha_{\text{Si-MgO}}^{\text{Si}}$	$\alpha_{\text{Al-SiO}_2}^{\text{Al}}$	$\alpha_{\text{Al-CaO}}^{\text{Al}}$	$\alpha_{\text{Al-MgO}}^{\text{Al}}$	$\alpha_{\text{Ca-SiO}_2}^{\text{Ca}}$	$\alpha_{\text{Ca-Al}_2\text{O}_3}^{\text{Ca}}$	$\alpha_{\text{Ca-MgO}}^{\text{Ca}}$	$\alpha_{\text{Mg-SiO}_2}^{\text{Mg}}$	$\alpha_{\text{Mg-Al}_2\text{O}_3}^{\text{Mg}}$	$\alpha_{\text{Mg-CaO}}^{\text{Mg}}$
A	.007159	.003451	.015136	.002350	.010836	.047529	.001586	.015174	.032082	.000563	.005390	.002598
B	.006762	.003961	.008905	.002774	.015131	.034018	.001320	.012297	.016192	.000345	.003214	.001882
C	.012945	.008785	.008816	.001428	.013486	.013534	.000742	.010325	.007032	.000521	.007251	.004921
D	.005974	.010258	.008125	.004460	.035412	.028050	.001853	.008567	.011652	.000284	.001315	.002258
E	.023574	.074877	.052942	.001270	.319358	.225806	.001306	.103388	.232189	.000260	.020599	.065429
F	.003502	.069512	.033009	.001918	.107902	.051238	.001491	.004224	.039822	.000455	.001288	.025575
G	.154598	.202696	.001582	.007520	3.369059	.026289	.005421	1.852427	.018952	.000106	.036309	.047606
H	.001589	.005776	.102235	.003779	.007476	.132334	.001796	.000978	.062909	.001584	.000862	.003133
I	.370031	.002200	.004109	.000120	.000497	.000929	.001247	.869364	.009653	.000160	.111619	.000664
J	.006557	.001733	2.315821	.006149	.008298	11.08943	.001284	.006557	2.315849	.003493	.017838	.004717

Table 14. Standard Deviations (σ) of the Twelve Empirical Alpha Factors Propagated by the Least Squares Solution of Ten Equations. (20 KV)

σ of the Following Alpha Factors:

	$\alpha_{\text{Si-Al}_2\text{O}_3}^{\text{Si}}$	$\alpha_{\text{Si-CaO}}^{\text{Si}}$	$\alpha_{\text{Si-MgO}}^{\text{Si}}$	$\alpha_{\text{Al-SiO}_2}^{\text{Al}}$	$\alpha_{\text{Al-CaO}}^{\text{Al}}$	$\alpha_{\text{Al-MgO}}^{\text{Al}}$	$\alpha_{\text{Ca-SiO}_2}^{\text{Ca}}$	$\alpha_{\text{Ca-Al}_2\text{O}_3}^{\text{Ca}}$	$\alpha_{\text{Ca-MgO}}^{\text{Ca}}$	$\alpha_{\text{Mg-SiO}_2}^{\text{Mg}}$	$\alpha_{\text{Mg-Al}_2\text{O}_3}^{\text{Mg}}$	$\alpha_{\text{Mg-CaO}}^{\text{Mg}}$
A	.008825	.004254	.018659	.000922	.004254	.018660	.000335	.003206	.006778	.000517	.004943	.002382
B	.024646	.014436	.032454	.000840	.004584	.010305	.000408	.003904	.005009	.000392	.003652	.002139
C	.007373	.005004	.008022	.001127	.010642	.010680	.000390	.005432	.003700	.000224	.003115	.002114
D	.009848	.016910	.013395	.001183	.009390	.007438	.000492	.002276	.003096	.000255	.001180	.002026
E	.009805	.031144	.022020	.000518	.130236	.092085	.000244	.019342	.043438	.000240	.019033	.060455
F	.002198	.043641	.020723	.000921	.051817	.024606	.000754	.002138	.020156	.000254	.000720	.014300
G	.123093	.161390	.001259	.003805	1.704672	.013302	.000783	.267494	.002737	.000090	.030775	.040351
H	.001825	.006636	.117456	.001290	.002552	.045167	.000721	.000392	.025256	.000792	.000431	.001568
I	.233920	.001391	.002597	.003231	.013393	.025011	.000175	.121833	.001353	.000289	.201398	.001197
J	.006902	.001824	2.437700	.004367	.005893	7.875751	.000281	.001433	.506363	.001639	.008371	.002212

Table 15. Standard Deviations (σ) of the Twelve Empirical Alpha Factors Propagated by the Least Squares Solution of Ten Equations. (30 KV)

σ of the Following Alpha Factors:

	$\alpha_{\text{Si-Al}_2\text{O}_3}^{\text{Si}}$	$\alpha_{\text{Si-CaO}}^{\text{Si}}$	$\alpha_{\text{Si-MgO}}^{\text{Si}}$	$\alpha_{\text{Al-SiO}_2}^{\text{Al}}$	$\alpha_{\text{Al-CaO}}^{\text{Al}}$	$\alpha_{\text{Al-MgO}}^{\text{Al}}$	$\alpha_{\text{Ca-SiO}_2}^{\text{Ca}}$	$\alpha_{\text{Ca-Al}_2\text{O}_3}^{\text{Ca}}$	$\alpha_{\text{Ca-MgO}}^{\text{Ca}}$	$\alpha_{\text{Mg-SiO}_2}^{\text{Mg}}$	$\alpha_{\text{Mg-Al}_2\text{O}_3}^{\text{Mg}}$	$\alpha_{\text{Mg-CaO}}^{\text{Mg}}$
A	.004432	.002136	.009370	.000694	.003202	.014046	.000265	.002540	.005371	.000517	.004943	.002382
B	.007284	.004267	.009592	.001135	.006189	.013914	.000241	.002242	.002952	.000228	.002125	.001245
C	.013604	.009233	.009266	.001026	.009691	.009726	.000398	.005538	.003772	.000128	.001783	.001210
D	.006424	.011032	.008738	.001631	.012947	.010255	.009880	.045683	.062139	.000390	.001803	.003096
E	.009369	.029760	.021042	.000535	.134565	.095146	.000298	.023574	.052943	.000182	.014439	.045861
F	.002643	.052476	.024919	.001432	.080555	.038252	.000703	.001991	.018771	.000292	.000828	.016442
G	.112711	.147778	.001153	.005788	2.593368	.020236	.000502	.171699	.001757	.000103	.035166	.046108
H	.000320	.001165	.020624	.001313	.002598	.045984	.000739	.000402	.025868	.000114	.000062	.000226
I	.284641	.001692	.003161	.009095	.037699	.070401	.000155	.108310	.001203	.000195	.136168	.000809
J	.005419	.001432	1.914079	.001235	.001666	2.226727	.000243	.001241	.438523	.002038	.010406	.002750

Table 16. Standard Deviations (σ) of the Twelve Theoretical Alpha Factors Propagated by the Least Squares Solutions of Ten Equations. (15 KV)

σ of the following Alpha Factors:

	$\alpha_{\text{Si-Al}_2\text{O}_3}^{\text{Si}}$	$\alpha_{\text{Si-CaO}}^{\text{Si}}$	$\alpha_{\text{Si-MgO}}^{\text{Si}}$	$\alpha_{\text{Al-SiO}_2}^{\text{Si}}$	$\alpha_{\text{Al-CaO}}^{\text{Al}}$	$\alpha_{\text{Al-MgO}}^{\text{Al}}$	$\alpha_{\text{Ca-SiO}_2}^{\text{Ca}}$	$\alpha_{\text{Ca-Al}_2\text{O}_3}^{\text{Ca}}$	$\alpha_{\text{Ca-MgO}}^{\text{Ca}}$	$\alpha_{\text{Mg-SiO}_2}^{\text{Mg}}$	$\alpha_{\text{Mg-Al}_2\text{O}_3}^{\text{Mg}}$	$\alpha_{\text{Mg-CaO}}^{\text{Mg}}$
A	$\sigma < 10^{-6}$	$\sigma < 10^{-6}$	1×10^{-6}	$\sigma < 10^{-6}$	$\sigma < 10^{-6}$	2×10^{-6}	$\sigma < 10^{-6}$	$\sigma < 10^{-6}$	2×10^{-6}	$\sigma < 10^{-6}$	1×10^{-6}	$\sigma < 10^{-6}$
B	$\sigma < 10^{-6}$	$\sigma < 10^{-6}$	$\sigma < 10^{-6}$	$\sigma < 10^{-6}$	$\sigma < 10^{-6}$	$\sigma < 10^{-6}$	$\sigma < 10^{-6}$	$\sigma < 10^{-6}$	$\sigma < 10^{-6}$	$\sigma < 10^{-6}$	$\sigma < 10^{-6}$	$\sigma < 10^{-6}$
C	$\sigma < 10^{-6}$	$\sigma < 10^{-6}$	$\sigma < 10^{-6}$	$\sigma < 10^{-6}$	$\sigma < 10^{-6}$	$\sigma < 10^{-6}$	$\sigma < 10^{-6}$	$\sigma < 10^{-6}$	$\sigma < 10^{-6}$	$\sigma < 10^{-6}$	$\sigma < 10^{-6}$	$\sigma < 10^{-6}$
D	$\sigma < 10^{-6}$	$\sigma < 10^{-6}$	$\sigma < 10^{-6}$	$\sigma < 10^{-6}$	$\sigma < 10^{-6}$	$\sigma < 10^{-6}$	$\sigma < 10^{-6}$	$\sigma < 10^{-6}$	$\sigma < 10^{-6}$	$\sigma < 10^{-6}$	$\sigma < 10^{-6}$	$\sigma < 10^{-6}$
E	$\sigma < 10^{-6}$	$\sigma < 10^{-6}$	$\sigma < 10^{-6}$	$\sigma < 10^{-6}$	$\sigma < 10^{-6}$	$\sigma < 10^{-6}$	$\sigma < 10^{-6}$	$\sigma < 10^{-6}$	$\sigma < 10^{-6}$	$\sigma < 10^{-6}$	$\sigma < 10^{-6}$	1×10^{-6}
F	$\sigma < 10^{-6}$	$\sigma < 10^{-6}$	$\sigma < 10^{-6}$	$\sigma < 10^{-6}$	$\sigma < 10^{-6}$	$\sigma < 10^{-6}$	$\sigma < 10^{-6}$	$\sigma < 10^{-6}$	$\sigma < 10^{-6}$	$\sigma < 10^{-6}$	$\sigma < 10^{-6}$	1×10^{-6}
G	1×10^{-6}	1×10^{-6}	$\sigma < 10^{-6}$	$\sigma < 10^{-6}$	7×10^{-6}	$\sigma < 10^{-6}$	$\sigma < 10^{-6}$	3×10^{-6}	$\sigma < 10^{-6}$	$\sigma < 10^{-6}$	1.1×10^{-5}	1.9×10^{-5}
H	$\sigma < 10^{-6}$	$\sigma < 10^{-6}$	2×10^{-6}	$\sigma < 10^{-6}$	$\sigma < 10^{-6}$	1×10^{-6}	$\sigma < 10^{-6}$	$\sigma < 10^{-6}$	2×10^{-6}	$\sigma < 10^{-6}$	$\sigma < 10^{-6}$	$\sigma < 10^{-6}$
I	7×10^{-6}	$\sigma < 10^{-6}$	$\sigma < 10^{-6}$	$\sigma < 10^{-6}$	$\sigma < 10^{-6}$	$\sigma < 10^{-6}$	$\sigma < 10^{-6}$	1.6×10^{-5}	$\sigma < 10^{-6}$	$\sigma < 10^{-6}$	2.2×10^{-5}	$\sigma < 10^{-6}$
J	$\sigma < 10^{-6}$	$\sigma < 10^{-6}$	17.3×10^{-5}	$\sigma < 10^{-6}$	$\sigma < 10^{-6}$	36.4×10^{-5}	$\sigma < 10^{-6}$	$\sigma < 10^{-6}$	17.2×10^{-5}	$\sigma < 10^{-6}$	$\sigma < 10^{-6}$	$\sigma < 10^{-6}$

Appendix 4. Miscellaneous Data

- I. CaO Problem
- II. Deadtime Corrections
- III. Drift Corrections

I. CaO Problem

The intensity ratios - $k_{\text{CaF}_2}^{\text{Ca}}/k_{\text{CaO}}^{\text{Ca}}$ and $k_{\text{CaCO}_3}^{\text{Ca}}/k_{\text{CaO}}^{\text{Ca}}$ - were measured at 10KV and 15KV:

	Ratio at 15 KV	Ratio at 10 KV
CaF_2/CaO	0.741	0.743
CaCO_3/CaO	0.537	0.555

In between the 15KV run and the 10KV run, the CaO mount was exposed to the air (by opening of the sample chamber, removal to the carbon coater and then return to the sample chamber for the 10KV run). If CaO reacts in the air to form Ca(OH)_2 and CaCO_3 , one might expect an increase in the ratios from the 15KV run to the 10KV run. The "contaminated" CaO (at the time of the 10KV run) would contain relatively less Ca than the "uncontaminated" (at the time of the 15KV run) CaO. It was impossible to tell whether such contamination was the only cause of the change in the ratios. Since the mount had had least exposure to air at the time of the 15KV run, these ratios were adopted for use in all of the alpha factor calculations.

II. Deadtime Correction

This correction was applied when count rate exceeded 10,000 cps.

10 KV Run: Count rate for Mg in MgO was approximately 20,000 cps.

15 KV Run: Count rate for Mg in MgO was approximately 30,000 cps.

Count rate for Ca in "CaO" (calculated from CaF_2 and CaCO_3) was approximately 14,000 cps.

20 KV Run: Count rate for Mg in MgO was approximately 40,000 cps.

Count rate for Ca in "CaO" was approximately 20,000 cps.

30 KV Run: Count rate for Mg in MgO was approximately 40,000 cps.

Count rate for Ca in "CaO" was approximately 30,000 cps.

Count rate for Si in SiO_2 was approximately 10,000 cps.

There were no deadtime corrections for any of the ten mixes.

III. Drift Corrections

- 10 KV Run: Mg counts (in MgO) were corrected for drift - the mean counts changed from 207,737 to 205,218 and were changed by increments of 252 per glass.
- 15 KV Run: No drift was observed.
- 20 KV Run: Si counts (in SiO₂) were corrected for drift by increments of 124 counts per glass out of approximately a total of 80,000 counts. Ca counts in "CaO" were corrected for drift by increments of 272 per glass out of a total of about 224,000 counts.
- 30 KV Run: Mg counts in MgO were corrected for drift by increments of 580 per glass. Total counts were approximately 400,000⁺.

REFERENCES

- Albee, A.L. and L. Ray, Correction factors for electron probe micro-analysis of silicates, oxides, carbonates, phosphates, and sulfates, *Anal. Chem.*, vol. 42, pp.1408-1414, 1970.
- Andersen, C.A. (ed.), *Microprobe Analysis*: New York, Wiley-Interscience, 1973.
- Bence, A.E. and A.L. Albee, Empirical correction factors for the electron microanalysis of silicates and oxides, *J. Geol.*, vol. 76, pp.382-403, 1968.
- Bevington, P.R., *Data Reduction and Error Analysis*: New York, McGraw Hill, 1969.
- Birks, L.S., *Electron Probe Microanalysis* (2nd ed.): New York, Wiley - Interscience, 1971.
- Castaing, R. and A. Guinier, *Electron microscope*, Proc. Delft Con., 1949.
- Yakowitz, H., Computational schemes for quantitative X-ray analysis: on-line analysis with small computers, in *Practical Scanning Electron Microscopy*, ed. by J. Goldstein and H. Yakowitz: New York, Plenum Press, 1975.
- Young, H.D., *Statistical Treatment of Experimental Data*: New York, McGraw Hill, 1962.
- Ziebold, T.O. and R.E. Ogilvie, An empirical method for electron micro-analysis, *Anal. Chem.*, vol. 36, pp.322-327, 1964.

FOUR STAR BRAND

SOUTHWORTH CO. L.S.A.

52% COTTON FIBER

PEGGY ANN DALHEIM